Carbon Dioxide injection into a partially-depleted gas condensate reservoir

A case study for optimal storage and re-use for field life-cycle extension through enhanced hydrocarbon recovery

J.J.F. Schut

Thesis committee:

Prof. Dr. P. L. J. Zitha (chair)
Dr. D. V. Voskov
Dr. A. Barnhoorn
Dr. M. W. van de Guchte

TU Delft

Carbon Dioxide injection into a partially-depleted gas condensate reservoir

A case study for optimal storage and re-use for field life-cycle extension through enhanced hydrocarbon recovery

by

J.J.F. Schut

In partial fulfilment of the requirements to obtain the degree of Master of Science
at the Delft University of Technology,
to be defended publicly on Friday December 1, 2017 at 10:00AM.

Student number:	4023781	
Project duration:	13 February, 2017 – 1 December, 2017	
Thesis committee:	Prof. dr. P. L. J. Zitha,	TU Delft, supervisor
	Dr. D. V. Voskov,	TU Delft
	Dr. A. Barnhoorn,	TU Delft
	Dr. M. W. van de Guchte,	Oranje-Nassau Energie B.V.

TU Delft Delft University of Technology

Acknowledgement

I would like to take this opportunity to thank my Supervisors, Pacelli Zitha and Denis Voskov, for their guidance and their brains to bounce ideas off of. Without the 2-weekly progress meetings a lot less detail would have gone into this case study. I would also like to thank Auke Barnhoorn, who was willing to be part of my committee late on in the project.

My sincere gratitude also goes out to Oranje-Nassau Energie (ONE) and the great enthusiastic workspace that it has offered me. I would like to thank the whole team for making this thesis project fun and memorable. Special gratitude goes out to my supervisors at ONE, Wisse van de Guchte, Jeroen Abels and Jeroen Mullink. Also, the professional experience of Wim van Vark, Barbara Schatz, Sander Kokxhoorn, Gerlof Visser, Reinoud Botman, Berend Vrouwe and Bart Kleimeer, has complemented this thesis in many ways. Thank you Alexander Berger for taking the time to have an introductory talk with me, that lead to a graduation topic that is very topical and interesting. I sincerely hope that my work and conclusions can be used to support decisions to be made for the future of Q16-Maas field.

Finally, but definitely not less important, I would like to thank my parents, without whom I would literally not be here. My mother for her grammatical check of the Thesis. And especially, my father, who's industry experience was instrumental for the quality of this case study as he offered interesting and useful insights.

Abstract

A pilot for a large scale, fully integrated chain of CO_2 capture, transport and storage (CCS) has been initiated in the port of Rotterdam. The initiative aims to demonstrate the technical and economic feasibility of CCS and show that it can be deployed on a large scale for power plants and energy-intensive industries that emit large volumes of CO_2.

The partially-depleted Q16-Maas gas condensate field could potentially be used to permanently store the captured greenhouse gas (CO_2). The case study shows the potential that this field has for CO_2 storage and also examines other options for life-cycle extension. The case study is based on macroscopic scale reservoir behaviour and simulated in the fully compositional simulator, Eclipse 300.

Gas reservoirs have a proven track record for safely trapping gaseous phases in the subsurface over long geological timescales. As long as initial reservoir conditions, mainly pressure (P_i=296,5 bar), are not exceeded, CO_2 in supercritical phase should be safely stored. According to literature, with increasing storage time, the CO_2 is even trapped more securely, although this process may take hundreds to thousands of years.

The results of the case study show that approximately 1.1 million tonnes of pure CO_2 can be stored in Q16-Maas field. By side-tracking the original well and producing the attic gas in the reservoir, 160 million cubic meters of additional gas can be recovered, along with condensate. If the side-tracked well is then converted to a CO_2-injection well, the CO_2 storage capacity is increased to 1.4 million tonnes. This injectable CO_2 volume is less than the two million tonnes originally estimated and this is due to the influx of water from a strong aquifer that has partially filled the void left by depleting the gas field.

The possibility of enhanced gas and condensate recovery using CO_2 has also been investigated in this case study, as the use of CO_2 for miscible floods in hydrocarbon reservoirs has been proven and used successfully as a tertiary recovery method. The reservoir simulation of the Q16-Maas field shows that there is no additional hydrocarbon recovery by CO_2 flooding. Sidetracking to and producing from an updip location in the reservoir is equally as productive. The reason for this is attributed to presence of a strong water aquifer, together with the varying reservoir quality and thickness prevents the successful application of CO_2 enhanced hydrocarbon recovery.

The total cost of transport and storage (OPEX and CAPEX) was estimated to be 71.5 million euro. Assuming CO_2 storage volume of 1.4 million tonnes, the project would need to receive roughly 50 euro/tonne in order to breakeven for storing and transporting the CO_2, the capturing is not included.

Table of Contents

List of Figures

List of Tables

1. Introduction

The goal of this case study is to find the optimal solution for the storage of CO_2 in the Q16-Maas field, while also considering enhanced hydrocarbon recovery options that could be economically feasible to pursue. Different variables will play a role in the determination of the optimal scenario. This chapter gives a brief introduction to the case study objective, the different facets of this research, discusses the reservoir simulator used and presents the research question.

1.1. Case Study Objective

Greenhouse emissions have been identified as one of the major contributors to the warming of the earth. The United Nations' Paris Agreement central aim is to strengthen the global response to the threat of climate change by keeping a global temperature rise this century well below 2 degrees Celsius above pre-industrial levels.

Europe's promise to lower greenhouse-gas emissions looked bright a dozen years ago, when its leaders created the first big market for trading carbon permits. Unfortunately, the system hasn't encouraged investment in clean technology as the cost of emitting carbon dioxide hasn't risen as expected.

The objective of the Emissions Trading System (ETS) was to cap the amount of emittable CO_2 and let companies receive or buy allowances according to their needs. Over time the emittable limit would be gradually reduced, causing a deficit in the market, that would drive up the CO_2 price. As years progressed and partly due to the financial crisis, the cap has hardly been adjusted and a remaining low carbon price has not encouraged investments for the shift to clean technology. (Bloomberg View, 2017) If the ETS were to eventually pick up and force companies to reduce the carbon emission, one of the options is to capture the CO_2 and store it in underground reservoirs, thus not emitting the carbon dioxide into the atmosphere. For this reason, pilots, like the ROAD project, are to be subsidized so that the storage of CO_2 in the subsurface can be tested and knowledge can be shared.

For its pilot, the ROAD project considers the Q16-Maas field that has been partially produced and has a strong aquifer presence. A case study needs to be conducted to investigate the different possibilities for further field usage. The resulting thesis topic reads:

Carbon Dioxide (CO_2) injection into a partially-depleted gas condensate reservoir: A case study for optimal storage and re-use for field life-cycle extension through enhanced hydrocarbon recovery.

The research questions that were analysed are:

1. Can CO_2 be contained within the reservoir safely? A literature review will be done to research the effect of CO_2 storage and the effects of injection on the different components within the reservoir.
2. Then, is a second up-dip well economically feasible?
3. The second up-dip well also brings the possibility of simultaneous injection and production to boost production potential, i.e. 'enhanced gas recovery' and 'enhanced oil recovery', from now on considered 'enhanced hydrocarbon recovery'.
4. The second up-dip well storage capacity is compared to the original well's storage capacity. The restrictions affecting the amount of storable CO_2 are also investigated as mitigating reaching the limitations can increase storage capacity.
5. Finally, a cost analysis for the different scenarios will be made to evaluate the different possibilities and determine the preferred strategy. This will also present a cost per volume CO_2 break-even price for this project.

The implementation and testing of different scenarios is done in a history matched compositional Eclipse model. The water influx effects and different producible layers have been best modelled in the simulation to ensure correct parameters pre-injection. A sensitivity analysis will be done to explore all the re-use and extensional scenario studies and consider a best match. The cost analysis of different scenarios will be discussed and estimated to give an idea of what carbon prices make CO_2 storage project economically viable.

1.2. ROAD

The ROAD (Rotterdam Capture and Storage Demonstration) project is an initiative of Uniper Benelux (previously E.ON Benelux) and ENGIE Energie Nederland (previously GDF SUEZ Energie Nederland). ROAD plans to capture 1.1 million tonnes of CO_2 per year from a new power plant at the Maasvlakte and will store the captured CO_2 into a depleted gas reservoir under the North Sea. ROAD aims to demonstrate the technical and economic feasibility of a largescale, integrated CCS chain deployed on power generation. Within the context of climate policy, CCS could make an important contribution to the reduction of CO_2 emissions. The knowledge and experience acquired within ROAD can be instrumental in the commercial introduction of CCS in the next decade. ROAD is co-financed by the European Commission within the framework of the Energy programme for recovery, the Government of the Netherlands and the Global CCS Institute. (Road2020.nl, 2017) The Q16-Maas gas condensate field is considered as the field for this storage pilot, as the first step. Subsequently, the project can use larger fields located further offshore.

1.3. Field location

The Q16-Maas field is located on the Dutch Continental Shelf offshore The Netherlands in the West Netherlands Basin, two km west of the Maasvlakte (onshore), see Figure 1. The apex of the field is located within the Q16c exploration licence and partly extends into the P18b and T01 offshore block as well as the onshore Botlek concession (Veenhof & Mullink, 2012). The field is operated by Oranje-Nassau Energie (ONE) with Energie Beheer Nederland B.V. (EBN), TAQA offshore B.V. (TAQA) and Energy06 Investments B.V. (EN06) as joint venture partners.

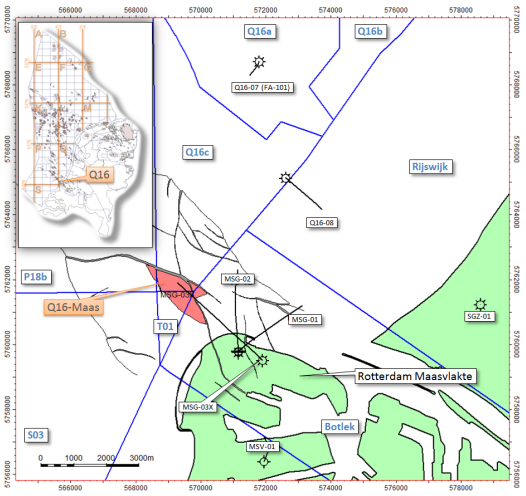

Figure 1. Overview of Q16-Maas block and concession boundaries

1.4. Enhanced Hydrocarbon Recovery

Hydrocarbon recovery efficiency can be increased by injecting miscible CO_2 gas in order to displace hydrocarbons towards producing wells. The process of enhanced oil/gas recovery can simultaneously and subsequently be used for CO_2 storage after economically recoverable hydrocarbons have been produced. According to Narinesingh & Alexander, gas condensate reservoirs provide possible storage sites, with the additional benefit of enhanced gas recovery through re-pressurization of the reservoir and re-vaporization of the condensate (Narinesingh & Alexander, 2014). This case study aims to review different recovery strategies and determine what re-use alternative is best suited for the Q16-Maas field, if any.

1.5. Reservoir Simulator - Eclipse

Eclipse is a widely-used industry standard commercial simulator. The Eclipse simulator suite consists of two separate simulators: Eclipse 100 (E100) specializing in black oil modelling, and Eclipse 300 (E300) specializing in compositional modelling.

Eclipse 100 is a fully-implicit, three-phase, three-dimensional, general purpose black oil simulator. Eclipse 300 is a compositional simulator with cubic equation of state, pressure dependant K-value and black oil fluid treatments. Eclipse 300 can be run in fully implicit, IMPES and adaptive implicit (AIM) modes. (Schlumberger, 2014) The default mode, implicit pressure and explicit saturation (IMPES), is used in this research as it is common practice.

Eclipse 300 has its own CO2STORE keyword. The keyword cannot be used due to the number of components included in the model, used for condensate blockage effects, together with the strong aquifer presence. Neither can an extension of this keyword be used. For this case study, the fraction of injected components was considered to be 100% pure CO_2.

1.6. Thesis Outline

Chapter 2 provides a literature review on CO_2 storage and how it is trapped within the reservoir. How gas condensate behaves when pressure depletes is researched along with enhanced hydrocarbon potential of CO_2 injection. Also, some other CO_2 storage/EOR projects are discussed and compared with the potential of this field.

The model and all the parameters put into the model are discussed in chapter 3. It also shows the differences that come with converting an E100 black oil to a compositional E300 model. The history matching of the field's production and pressure behaviour is matched until January 1st 2017.

Chapter 4 expands on chapter 3 and looks into the option of sidetracking from the current well MSG-03X and producing from the attic gas that may still be present updip from the current well location.

CO_2 injection is investigated for the forecast cases with and without sidetrack in chapter 5. Different bottomhole pressure (BHP) limits are tested to see the full potential of storage volume.

The combination of production and injection to mobilize condensate dropout is studied in chapter 6. As the field consist of multiple reservoir layers with different parameters a couple of scenarios can be tested.

In chapter 7 all the data from chapters 4 until 6 are compared and an economic review is done for each relevant scenario. Within this chapter, a break-even carbon emission price is calculated for the scenario with the highest potential and with it, the additional costs for CO_2 injection are discussed.

Chapter 8 provides concluding remarks and a discussion of the case study. Further research is also proposed.

2. Literature Review

One of the measures to reduce emissions of carbon dioxide into the atmosphere is to implement carbon capture and storage (CCS). Gas reservoirs have a proven track record for the safe trapping of gaseous phases in the subsurface over long geological timescales. This makes these types of sites potentially interesting for CO_2 storage. The injection of CO_2 into a formation can also have the added benefit of enhancing hydrocarbon recovery. The combined CO_2 storage and enhanced hydrocarbon recovery of partially depleted gas condensate reservoirs has not been subject to extensive research for existing field developments. Each following subchapter elaborates and expands on the existing research on the subject of CO_2 storage and CO_2 enhanced hydrocarbon recovery relevant for a partially depleted gas condensate reservoir.

2.1. CO_2 storage

2.1.1. CO_2 Behaviour in Reservoirs

The CO_2 will generally be injected underground as a so-called supercritical fluid. This term means that the CO_2 has a liquid-like density and flows like a gas. With decreasing pressure, it will expand and form a gas without phase transition (it will not boil) (Blunt, 2010). CO_2 is supercritical at pressures and temperatures exceeding its critical pressure (7.3773MPa = 73.8 bar) and temperature (30.978°C) (Span & Wagner, 1996). As a rule of thumb CO_2 can considered to be supercritical at depths greater than 800 meters, assuming a hydrostatic pressure gradient of 0.1bar/meter. At depths exceeding two kilometres the density of supercritical CO_2 can be considered stable, see Figure 2 (Tan, 2012). Figure 2 also shows the large volume reduction CO_2 undergoes when exposed to higher pressures, with increasing depth. A specific volume of CO_2, at the surface i.e. atmospheric pressure, will roughly be reduced by a factor of $370 \left(= \frac{100}{0.27}\right)$ when it reaches depths of two kilometres.

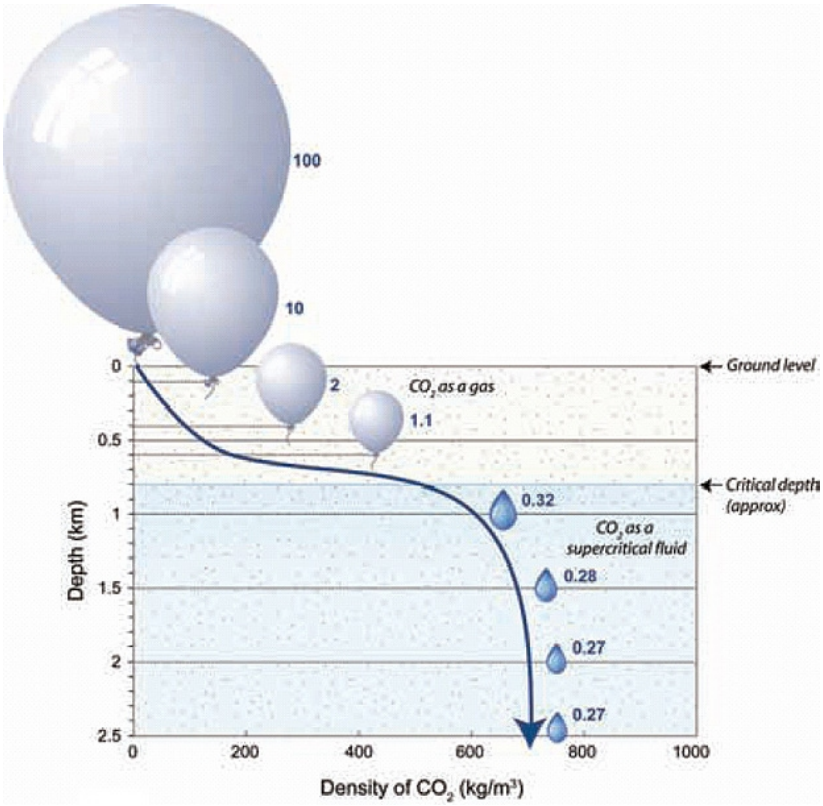

Figure 2. Relationship showing density vs. depth of CO_2; (Global CCS Institute, 2009)

What this essentially means is that CO_2 in supercritical form allows for larger storage volumes than in gaseous form because of the shrinkage factor. The density of CO_2 that comes with the high pressures and temperatures (±700kg/m^3) within a reservoir is lower than that of the formation water (±1000kg/m^3) and will cause it to 'float' on top the water that is present.

The buoyancy effect of the CO_2 is a vital component in the trapping of CO_2 in the subsurface. As we are interested in long term trapping of the CO_2, it is imperative that CO_2 cannot escape. (Blunt, 2010) There are four main trapping mechanisms: structural & stratigraphic, residual, solubility and mineral trapping (Price & Smith, 2008).

2.1.2. Trapping Mechanisms

Hydrocarbon reservoirs have already shown their ability to trap gasses and liquids for long periods of time. An impermeable cap rock is essential to prevent upwards movement of CO_2 and form a continuous primary seal. In *stratigraphic trapping*, cap rock forms a closed container to trap the CO_2. In *structural trapping*, impermeable rocks shifted by a fold or fault in the geologic strata hold the CO_2 in place. Examples of such traps are given in Figure 3.

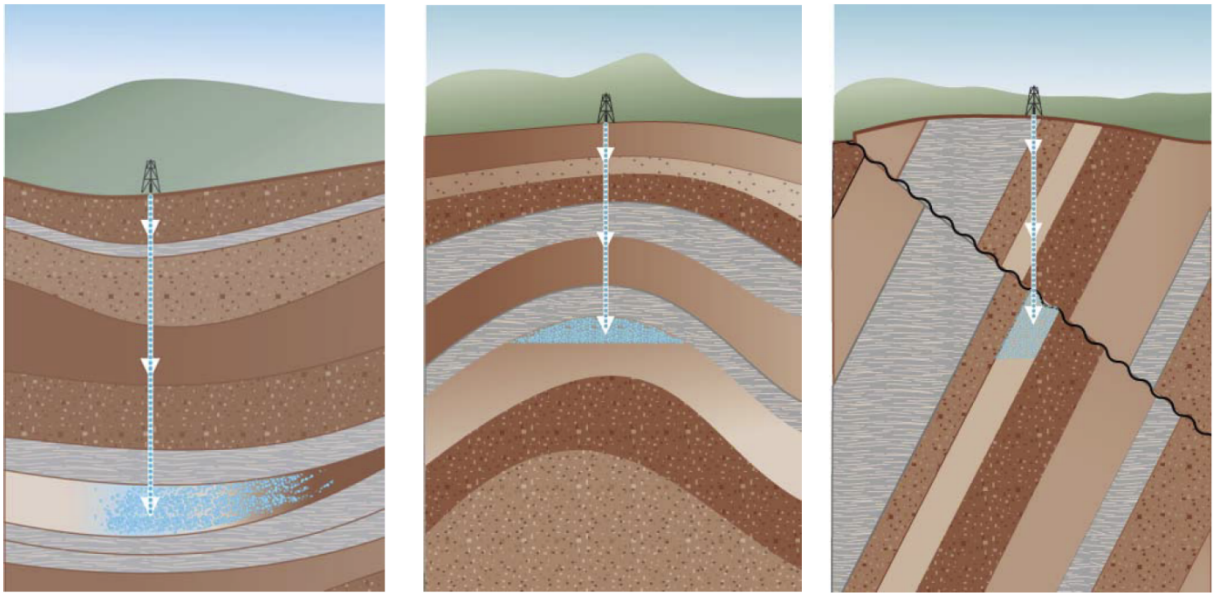

Figure 3. Examples of stratigraphic (left) and structural (middle and right) trapping; (Price & Smith, 2008)

Over time the trapping mechanisms increase with storage security. In *residual trapping*, which usually begins after injection is stopped, the CO_2 is trapped in tiny pores in the formation by the capillary pressure of water. Formation water returns to the pores now containing CO_2. As this happens, the CO_2 becomes immobilized by the pressure of the added water.

With *Solubility trapping* the CO_2 dissolves into the saline water. This process takes hundreds to thousands of years. The safest trapping mechanism is *mineral trapping*. In some formations, dissolved CO_2 may react chemically with the surrounding rock formations and form solid, stable minerals, for example $CaCO_3$, $MgCO_3$ of $FeCO_3$. This is an extremely slow process that will take thousands of years (Price & Smith, 2008). A trapping overview is given in Figure 4.

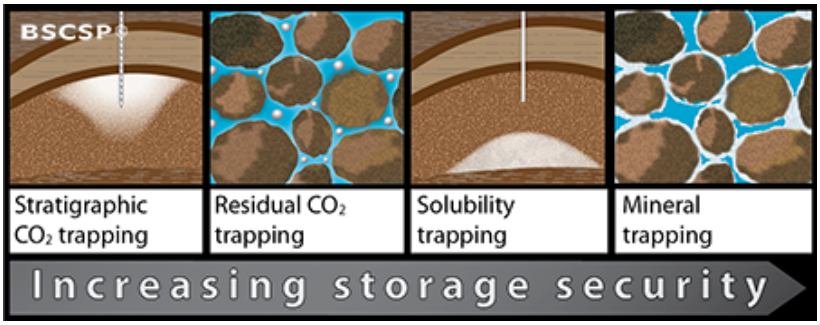

Figure 4. Different trapping mechanisms with increasing storage security over time; (http://www.bigskyCO_2.org/node/127)

2.2. Gas Condensate Reservoirs and Condensate Blockage

There are three types of gas reservoirs: dry gas, wet gas and gas condensate reservoirs. A gas condensate is single-phase at original reservoir conditions. It predominantly is built up of methane [CH_4] and other short-chain hydrocarbons, but also contains long-chain hydrocarbons, termed heavy ends. As a reservoir is produced, the pressure drops, while the average temperature stays relatively unchanged (isothermal). This decrease in pressure causes the single-phase to pass through the dewpoint, the point at which liquid starts to drop out of the gas. A gas that separates into two phases, a gas and a liquid, is called retrograde condensate (Fan, et al., 2005). This is shown in the phase diagram in Figure 5.

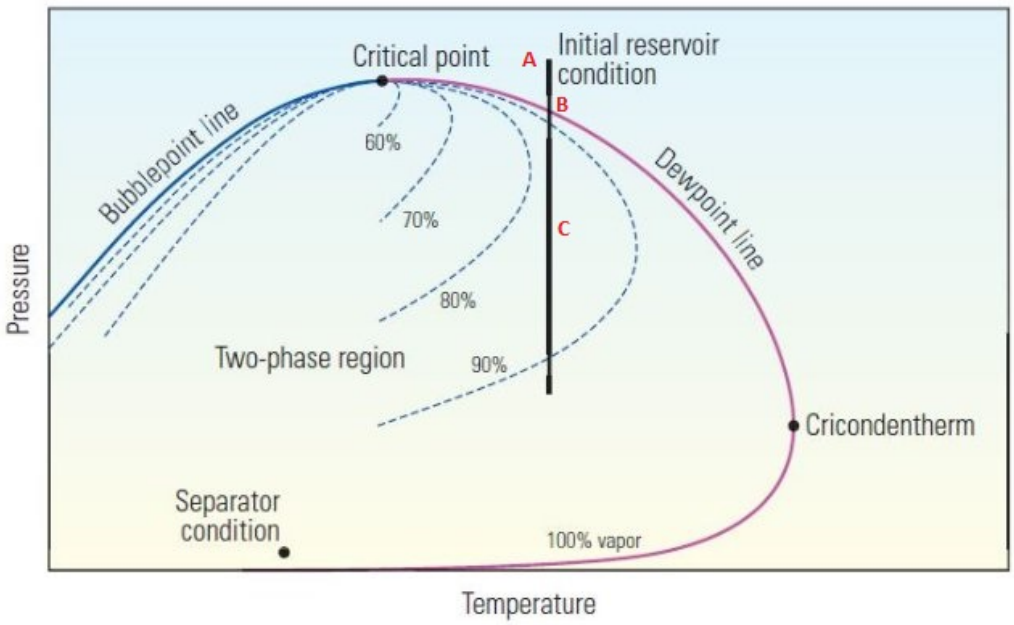

Figure 5. Phase diagram example of gas condensate system; (Fan, et al., 2005)

The black line seen in Figure 5 shows the phases that a gas condensate goes through as gas from a reservoir is produced. The initial reservoir condition of a gas condensate is shown in point A. As the gas is produced, the pressure decreases. Until point B the gas condensate is a single-phase gas.

The retrograde condensate, rich in heavy ends, drops out of the solution at point B, as the gas condensate passes the dewpoint line. With decreasing pressure even more condensate drops out into the reservoir, to a maximum volume fraction of roughly 17% condensate (83% vapour) for this gas condensate, at point C. Eventually, as pressure decreases further, re-vaporization of the retrograde liquid starts to occur.

The dewdrops are less mobile than the gas because of capillary forces acting on the fluids. Consequently, some of the condensate that forms in the reservoir is left behind. The biggest pressure drop in a reservoir is near to the wellbore. After a transient period, the accumulation of liquids around the wellbore is enough to mobilize the liquid. The consequences of reservoir pressure dropping below the dewpoint pressure has two results, both negative: gas and condensate production decrease because of near-well blockage, due to condensate dropout, and the produced gas contains fewer valuable heavy ends because of dropout throughout the reservoir, where the condensate has insufficient mobility to flow towards the well (Fan, et al., 2005).

The condensate blockage effects are shown in Figure 6. The condensate saturation, S_o, is highest near the wellbore because the pressure is lower, which means more liquid dropout. The condensate/oil relative permeability, k_{ro}, increases with saturation. The decrease in gas relative permeability, k_{rg}, near the wellbore illustrates the blockage effects.

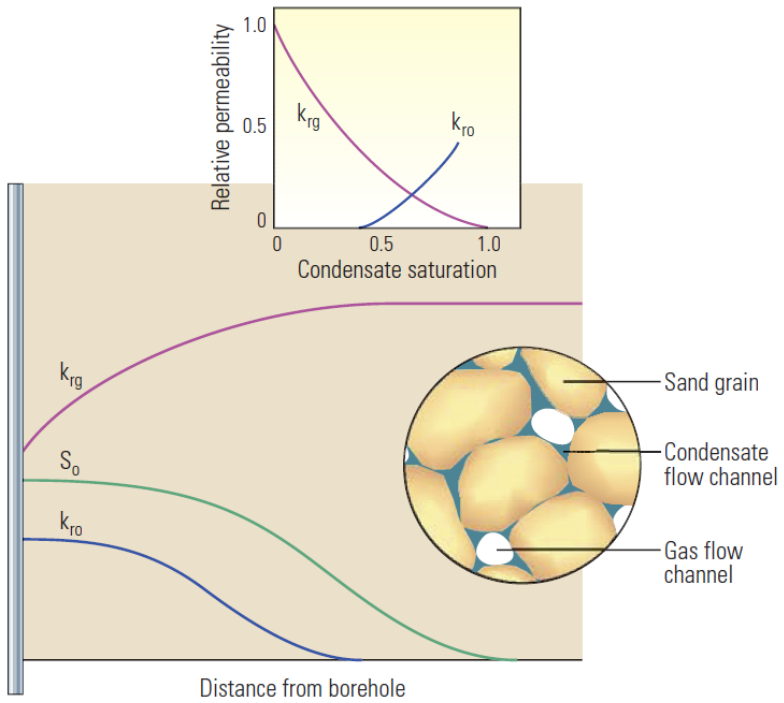

Figure 6. Condensate blockage effect; (Fan, et al., 2005)

Gas condensate field behaviour can be divided into three regions once bottomhole pressure, P_{BH}, drops below the dewpoint pressure, P_D. Figure 7 shows the three regions. Region 3 is the region where the reservoir pressure exceeds the dew point pressure. In this region only one hydrocarbon phase is present. Closer to the well, in region 2, the condensate build-up occurs as liquid drops out of the gas phase. The liquid saturation is still too low for it to mobilize. There is only single phase gas flow in this region. In region 1, closest to the producing well, the gas condensate saturation is largest. Both phases flow here.

These regions can be linked back to the relative permeability curves in Figure 6. In region 3 the single phase gas is not influenced by the relative permeability curves because the condensate saturation is zero. In region 2 the condensate saturation is low. At this point the relative permeability of the condensate is close to zero and thus immobile. In region 1 the relative permeability of the condensate will be larger than zero and will mobilize.

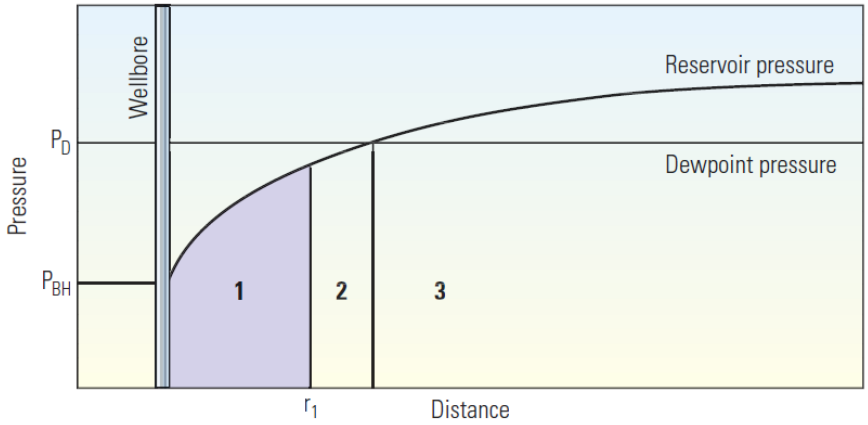

Figure 7. Three gas condensate reservoir regions; (Fan, et al., 2005)

2.3. Enhanced Hydrocarbon Recovery by means of CO_2 Injection

Injecting carbon dioxide into oil reservoirs for enhanced oil recovery has been practiced on a commercial scale for nearly 50 years, with the first successful pilot tests conducted in the early 1960s in the state of Texas (IEA, 2015). Well productivity declines in gas condensate reservoirs is usually caused by condensate blockage as the reservoir pressure declines (Fan, et al., 2005). Re-pressurizing the reservoir can vaporize condensed hydrocarbon and alleviate condensate blockage (Narinesingh & Alexander, 2014). In the supercritical phase, CO_2 can be very effective at condensate recovery as it will re-pressurize the hydrocarbons into a more mobile phase. It also minimises the surface tension that exists between the gas and liquid phase and frees the trapped condensate (Kurdi, Xiao, & Liu, 2012).

Increased recoveries have been the driving force behind the use of CO_2. Assuming enhanced oil production can be combined with CO_2 sequestration, this remains an attractive option for the medium to longer term, particularly if the current trend of rising energy demand and increasing CO_2 emissions continue (Shtepani, 2006).

2.4. Ongoing Carbon Capture and Storage Projects

Carbon Capture and Storage is not something new, it is proven and in use around the world. CO_2 is primarily used as an enhanced oil recovery method. Currently, there are 21 large-scale CCS projects in operation or under construction globally. Combined, these projects have a capture capacity of 40 million tonnes of CO_2 per year (Mtpa) (Global CCS Institute, 2016a).

In the Netherlands, CO_2 has been injected in the subsurface since May 2004. The field in question is the K12-B gas field located in the Dutch sector of the North Sea. The natural gas produced has a high CO_2 content (13%) and the CO_2 is separated prior to gas transport to shore. The CO_2 used to be vented into the atmosphere but is now injected into the field above the gas-water contact. K12-B is the first site in the world where CO_2 is injected into the same reservoir from which it originated. The field is still producing today, but is nearly depleted (Vandeweijer, et al., 2011).

Sleipner is the first large scale commercialized CCS project. The gas and condensate fields are located off the coast of Norway in the North Sea. Since operation began in 1996, the Sleipner project has a total storage volume potential of 17.5 million tonnes of CO_2 into a saline aquifer located about 800-1000 meters beneath the seabed (Global CCS Institute, 2016b).

The Weyburn-Midale carbon dioxide project is considered the largest full-scale CCS field study ever conducted. The combined amount of CO_2 estimated to be injected in the two fields is 40+ million

tonnes (Zaluski, El-Kaseeh, Lee, Piercey, & Duguid, 2016). The study covers the mile-deep seal containing the reservoir, CO_2 plume movement and the monitoring of permanent storage. CO_2 from the 'Great Plains Synfuels' plant in the United States is captured and transported across the border into Saskatchewan, Canada since 2000 (PTRC, 2014).

In 1993, the European Commission began the Joule II Non-nuclear Energy Research Program, which studied sequestration of industrially produced CO_2 (Holloway, 1996). The Joule II study concluded that (i) shallow reservoirs do not provide sufficient storage for carbon dioxide because it would be in gaseous form, (ii) for maximum storage capacity, carbon dioxide has to be stored as a supercritical fluid - which requires reservoirs deeper than 800 m (2,600 ft), (iii) such deep reservoirs could be depleted oil or gas reservoirs or structures containing aquifers, (iv) if carbon dioxide is stored in aquifers, then to avoid contaminating shallower potable water sources, carbon dioxide would be sequestered in aquifers deep below the North Sea, (v) if carbon dioxide is injected into a limestone reservoir, carbonate dissolution could occur around the injection wells causing subsidence, and (vi) the cost of carbon dioxide separation out of flue gas is significantly higher than that of transporting and injecting carbon dioxide in reservoirs (Seo, 2004).

2.5. Q16-Maas Field's Potential for CO_2 Storage and Enhanced Gas and Condensate Recovery

The gas field operated by Oranje-Nassau Energie off the coast of the Netherlands may be a perfect test reservoir for carbon dioxide storage. The Q16-Maas field is a condensate-rich field located just offshore the Maasvlakte, in the Rotterdam harbour area. Being near to the coast it has been drilled from an onshore location which has the extra benefit of reduced expensive transportation costs. The CO_2 is captured nearby in the E.ON power plant. Initially a field 20km offshore was planned for this project but due to the financial gap caused by structural low carbon prices, ROAD had to review its project set-up.

'Rotterdam Opslag en Afvang Demonstratieproject' (ROAD, translated: Rotterdam Storage and Capture Demonstration Project) is the collective name for the initiators of this project. A planned storage capacity of 1.1 million tonnes annually of CO_2 is planned for 2 years. It is one of the first projects that will incorporate all the different facets of the CCS chain. It will be a project that aims to demonstrate the technical and economic feasibility of CCS. The knowledge and experience acquired within ROAD can be instrumental in the commercial introduction of CCS. ROAD is co-financed by the European Commission within the framework of the Energy programme for recovery, the Government of the Netherlands and the Global CCS Institute (Road2020.nl, 2017).

3. Reservoir Model

The model used for this case study is a static model using interpreted seismic and well logs of the Q16-Maas gas-condensate field. As this field has already been chosen for a possible carbon capture and storage pilot in the Netherlands, the findings of this case study can be compared and used to re-evaluate if CO_2 can be stored in other comparable fields. This chapter supplies information about the field that can eventually be used as a representative case study for a gas-condensate field with aquifer influx. Also, all the relevant data is shown and certain modelling decisions are substantiated. The study is done on a macroscopic scale.

3.1. Static Model

The Maasgeul-03X (MSG-03X) exploration well was drilled in the summer of 2011 and converted into a production well in 2014. Initially, only the Hardegsen interval was perforated; in a later stage the Röt and Detfurth formations were also perforated. Production started on the 29th of April 2014. Figure 8 shows an overview of the 3D static model of the field.

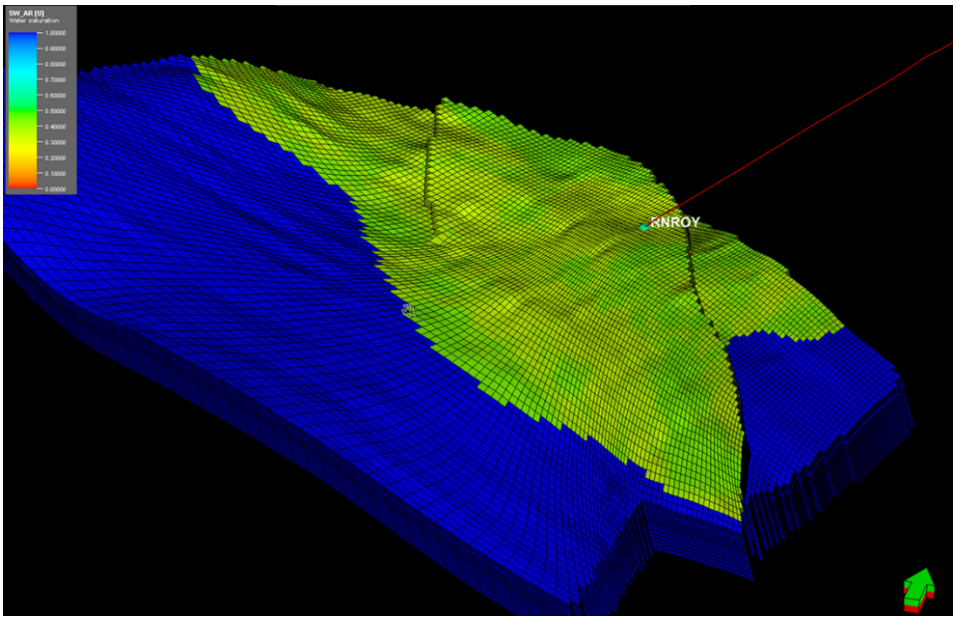

Figure 8. Q16-Maas static model showing water saturation, top Röt siltstone; (Oranje-Nassau Energie, 2017)

The field consists of three fault blocks that are depicted by different segments, as shown in Figure 8. All the segments within the Maas field retain reservoir-to-reservoir contact through different layers, for example the Hardegsen of the main block juxtaposes the Röt of the western fault block. The Bunter sandstones (Hardegsen, Detfurth and Volpriehausen) consist of massive sandstones that are interpreted to be braided stream deposits which grade upwards into sand- and siltstones of the Lower Röt formation, shown in Figure 10. The initial estimates showed a gas initially in place (GIIP) of roughly 1 Bcm in the (main) Bunter reservoir, while the Röt contains an estimated 0.3 Bcm, of which a large proportion is deemed not producible due to poor reservoir quality.

3.1.1. Well Data

Complementary to the static geological model, the well data and core samples are essential for the correct modelling of reservoir. Figure 10 shows the wireline data and core sample data combined. The Upper Hardegsen shows very high permeability and porosity, in both wireline and core data. The quality of the reservoir layers, as depicted in the Figure 10, decreases with increasing depth. The gas-water contact is interpreted at a depth of 2898m TVDss and is based on the high water saturation value that comes with it, together with the RFT data shown in Figure 9.

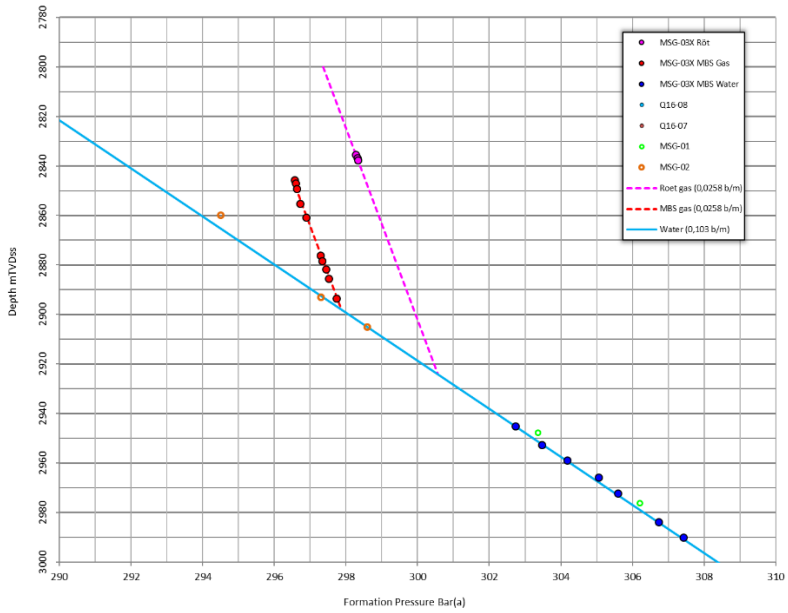

Figure 9. Gas gradients and water gradient for GWC determination

The Röt consists of two layers, of which the siltstone is of poor quality and is considered not producible. The deeper sandstone layer is thin, and of far lesser quality than the Hardegsen, but still contains hydrocarbons that can be accessed from the same well.

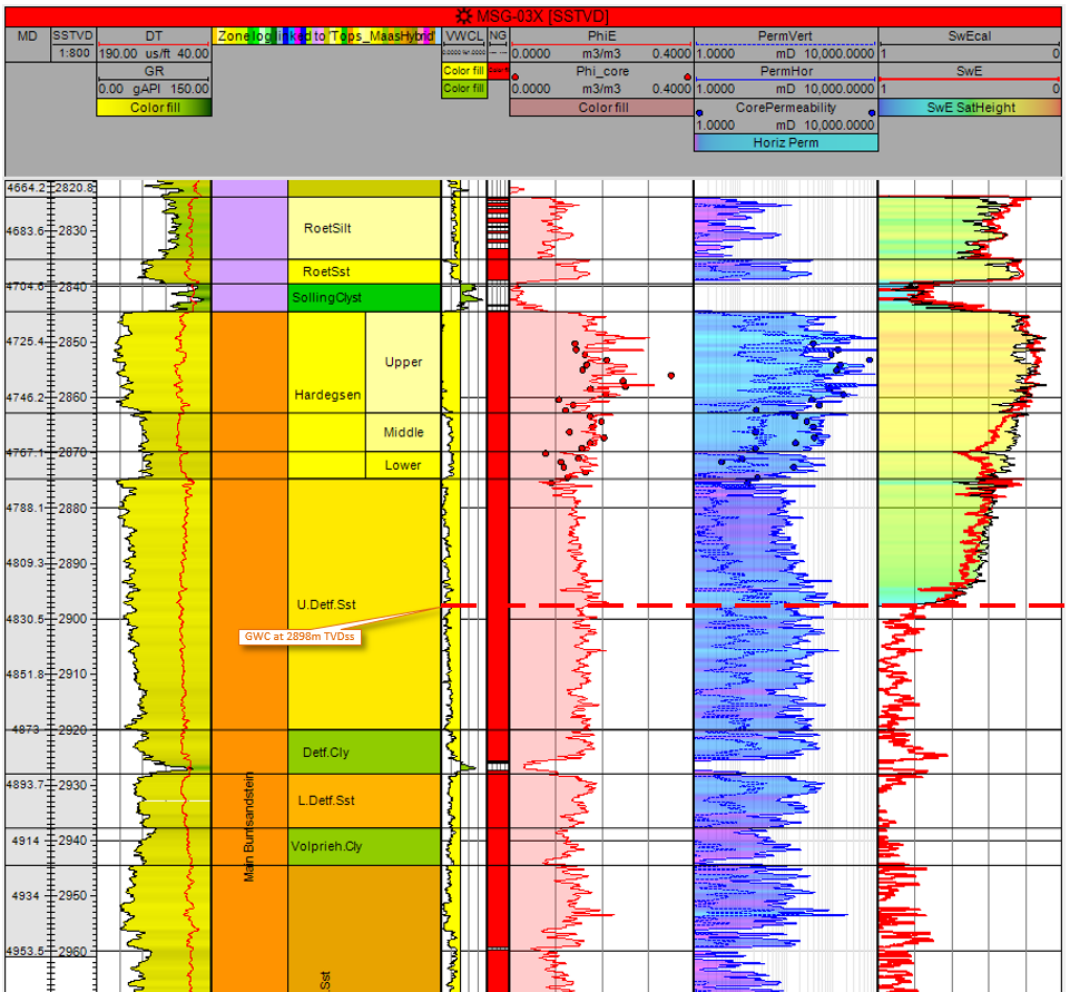

Figure 10. Petrophysical evaluation of MSG-03X; (Oranje-Nassau Energie, 2017)

3.2. Dynamic Model

The initial static model (built in Petrel) consisted of over 3 million gridblocks and also included a neighbouring field. A reduced version of the initial static model was used, shown above in Figure 8, as the basis to build a dynamic model in Eclipse. An analytical aquifer was then attached to the southern flank of the model. This way, the number of grid blocks was reduced in order to keep computational duration as short as reasonable possible. The dynamic model is used to history match the field behaviour.

3.2.1. Well Interventions

From well tests, it was concluded that the productivity of the Upper Hardegsen is very high. The average permeability of the perforated interval is ±300mD. The highest permeability layers were intentionally not perforated as to mitigate sand production.

Initially, the Röt formation was not perforated as its pressure exceeded that of the Bunter reservoir which was of much better quality. The Solling Claystone between the Bunter reservoir and Röt offers an impermeable layer between the two. In April of 2016, the Lower Röt (which is of better quality than the Upper part) was perforated in order to prolong the production plateau and delay the need for compression. The Lower Hardegsen and Upper Detfurth intervals were opened in June 2016, after logs had confirmed there to be bypassed gas behind casing. These consisted of a Production Logging Tool (PLT) and Memory Pulsed Neutron-Neutron (MPNN) logging tool that were run to investigate the inflow performance of the different perforated zones (run on the 1st of June). This was repeated later, on the 9th of October, as water production increased. The increase in water production (>450Nm3/day) exceeded the capacity of the surface facilities, requiring the Hardegsen and Detfurth zones to be permanently plugged off in October 2016. Since then the field has only been producing from the Röt formation. Figure 11 shows a simplified sketch of the well's interventions over time, and does not consider gas-water contact (GWC) level changes.

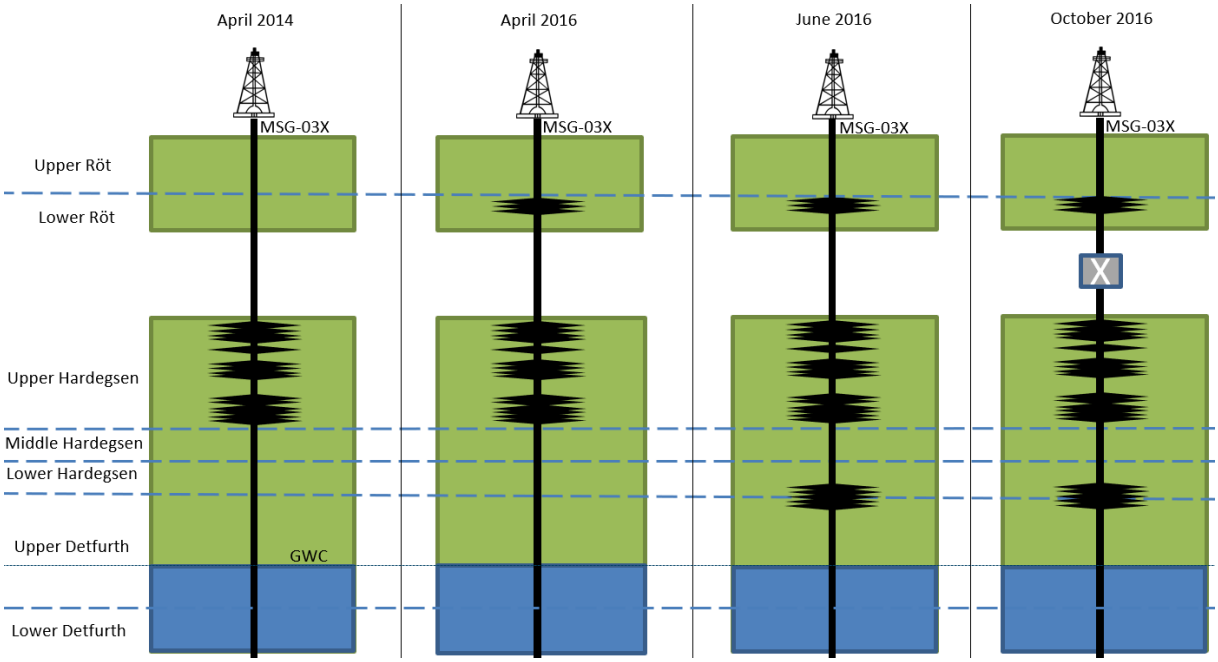

Figure 11. Simplified sketch of well interventions over time

3.2.2. Production Logging Tool Data

The PLT data that was acquired gives a good indication of where the water and gas comes from after the Röt is perforated. The first PLT/MPLT was run on the 1st of June 2016 and the obtained data is summarised in Table 1, below. Each perforated section has an overall flow rate and specific flow rates of liquids and gas. The actual logs are shown in Appendix A.

1st June 2016	Gas			Water			Total Flow
Zones	Surface	Downhole	Zonal %	Surface	Downhole	Zonal %	Zonal%
Total	431.92 Mm^3/d	2110.32 Mm^3/d	100.00%	102.06 m^3/d	106.20 m^3/d	100.00%	100.00%
Röt (4694 - 4704m MD)	133.01	649.74	30.79%	1.17	1.23	1.16%	29.45%
Hardegsen 1 (4715 -4723m MD)	263.83	1289.37	61.10%	19.42	20.18	19.0%	59.17%
Hardegsen 2 (4725 -4727.5m MD)	33.91	166.03	7.87%	22.08	22.97	21.63%	8.49%
Hardegsen 3 (4733.5 -4723m MD)	0.23	1.06	0.05%	9.80	10.19	9.60%	0.49%
Hardegsen 4 (4742.5 -4766m MD)	0.94	4.12	0.20%	49.59	51.63	48.62%	2.40%

Table 1. PLT/MPLT data for different reservoir zones on June 1st 2016

From Table 1 it can be seen that the majority of gas production (61.1%) was coming from Hardegsen 1 and the Röt (30.8%). The majority of the water production was coming from Hardegsen 4 (48.6%) and Hardegsen 2 (21.6%) with hardly any water production from the Röt.

9th October 2016	Gas			Water			Total Flow
Zones	Surface	Downhole	Zonal %	Surface	Downhole	Zonal %	Zonal%
Total	116.40 Mm^3/d	555.83 Mm^3/d	100.00%	310.35 m^3/d	322.92 m3/d	100.00%	100.00%
Röt (4694 - 4704m MD)	56.73	272.41	49.01%	16.0	16.64	5.15%	33.39%
Hardegsen 1 (4715 -4723m MD)	54.57	260.84	46.93%	101.62	105.73	32.74%	41.89%
Hardegsen 2 (4725 -4727.5m MD)	1.01	2.08	0.73%	81.17	84.47	26.16%	9.80%
Hardegsen 3 (4733.5 -4723m MD)	0.04	0.16	0.03%	2.62	2.73	0.85%	0.32%
Hardegsen 4 (4742.5 -4766m MD)	4.05	18.34	3.30%	108.94	113.36	35.10%	14.64%

Table 2. PLT/MPLT data for different reservoir zones on October 9th 2016

Table 2 shows the results from the PLT run on October 9th. If Table 1 is compared to Table 2 some clear changes can be noticed:

- The water production increases 3-fold, while gas production decreases to a quarter of its previous rate.
- The majority of gas produced still mainly comes from the Röt (49.0%) and Hardegsen 1 (46.9%) although the shift in percentage is quite significant after only four months of production. This is mainly due to the significant increase in water production from the Hardegsen 1 zone (32.74%). Other big contributors to the water production are from the Hardegsen 4 (35.1%) and Hardegsen 2 (26.16%).

Shortly after running the PLT log it was decided to plug off the Hardegsen due to the large amount of water production. Since then only the Röt has been produced. Production shows increasing skin effects, most likely due to condensate banking occurring in the low permeable formation.

3.2.3. History Match

As previously mentioned, two different formations contain gas. When considering production history, shown in Figure 12, one can clearly see the significant increase in water production after the Röt perforation in April 2016. The increased water production can restrict the amount of hydrocarbon production as the well starts to load up, causing increased bottom hole flowing pressure. The maximum amount of water production of 450m^3/day is reached in October 2016, consequently the Hardegsen and Detfurth were plugged off. The water production is considered to be one of the most important history match parameters.

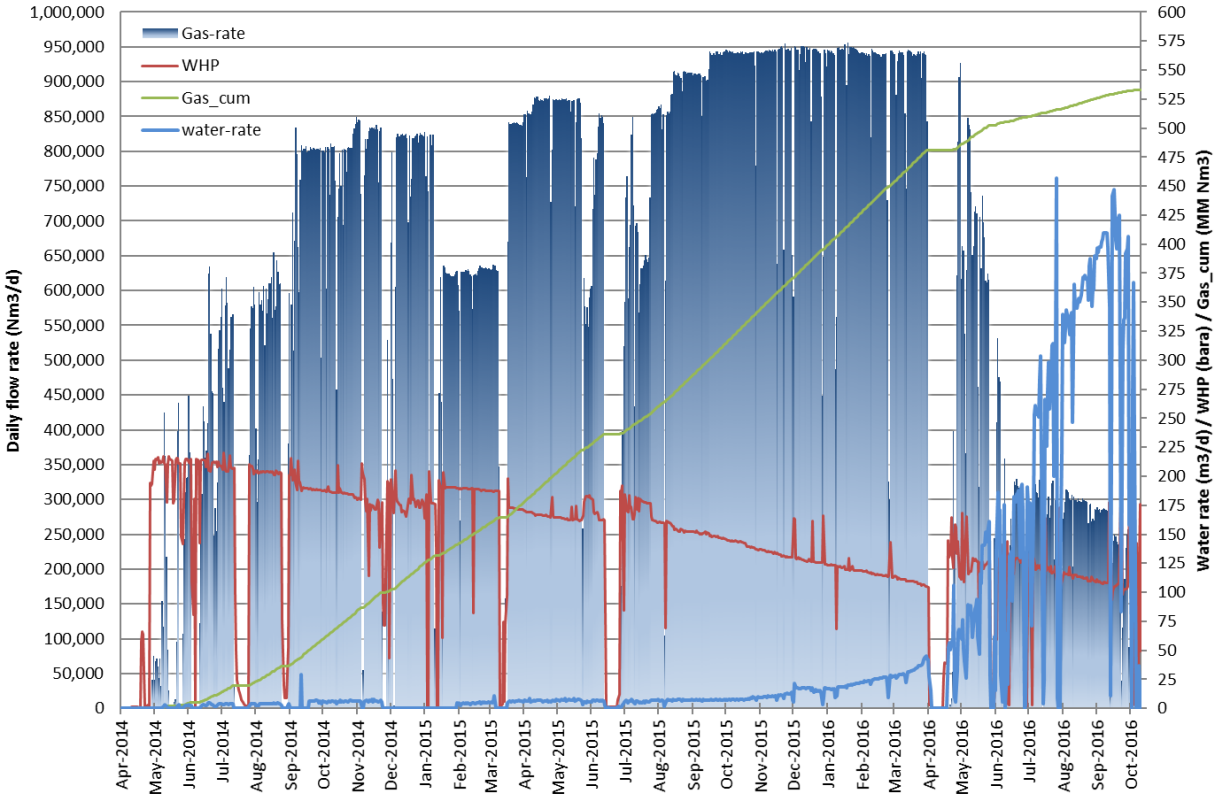

Figure 12. Q16-Maas gas production including wellhead pressure, cumulative gas production and water production rate

3.2.4. Fetkovitch Aquifer

Since the pressure of the reservoir did not decline as much as was expected with production, and given the large increase in water production that was noticed, it is believed that a strong aquifer is connected to the reservoir. The aquifer is a large source of water that provides pressure support and causes water influx into the reservoir. The aquifer size and strength were analytically determined using material balance calculations for Fetkovitch aquifers. (Dake, Volume 8, 1st edition)

Using the method of Fetkovitch, the following two equations are required:

Equation 1. $$\bar{p}_{a_{n-1}} = p_i\left(1 - \frac{\sum_{j=1}^{n-1}\Delta W_{e_j}}{W_{ei}}\right)$$

Equation 2. $$\Delta W_{e_n} = \frac{W_{ei}}{p_i}\left(\bar{p}_{a_{n-1}} - \bar{p}_n\right)\left(1 - e^{-J_{P_i}\Delta t_n / W_{ei}}\right)$$

For which

Equation 3. $$W_{ei} = \bar{c}\, W_i p_i$$

Fetkovitch's equations calculate the void replacement, i.e. the water influx replacing the gas produced, as a function of time and pressure. The aquifer size $[W_i]$ and aquifer productivity index $[J]$ are unknown and by means of plotting cumulative water influx $[W_e]$ with substantiated guesses for the two variables, one can find a best estimate for these values. The intermediate results are shown in Table 3. The initial reservoir pressure $[p_i]$ is taken to be 296,5 bar and the total pore compressibility is calculated to be 7,25E-05 bar^{-1}, assuming:

$$[\bar{c} = c_w + c_f = 2.90E-05\frac{1}{bar} + 4.35E-05\frac{1}{bar}].$$

Step	Date	Time	Pres				
n			p_n	$p_{a,n-1}$-p_n	$\Delta W_{e,n}$	$W_{e,n}$	$p_{a,n}$
-		years	bar	bar	MMm^3	MMm^3	bar
0	1-apr-14	0,00	296,5	296,5		0,000	297
1	25-Nov-14	0,65	277,3	19,2	0,218	0,218	291
2	12-Mar-15	0,95	266,8	25	0,136	0,354	288
3	26-Jun-15	1,24	258,6	30	0,163	0,517	285
4	12-Apr-16	2,03	222,4	62	0,836	1,352	265
5	31-May-16	2,17	226,0	39	0,103	1,456	263
6	10-Oct-16	2,53	234,2	29	0,193	1,649	259

Table 3. Fetkovitch pressure and influx results

Table 3 shows the dates of each known pressure measurement together with the accompanying pressure measured $[p_n]$. The difference in water influx $[\Delta W_e]$ for each time step is then calculated with equation 2, for which W_i needs to be guessed (linked with equation 3). The cumulative water influx, shown in the second to last column can then be taken for each time step. Lastly, the average pressure in the aquifer is calculated with the change in aquifer volume, see equation 1. The calculated aquifer influx should then be plotted and align with the known void replacement. The resulting aquifer size $[W_i]$ was 600mln rm^3(reservoir cubic meters) and aquifer productivity index $[J]$ of 55m^3/d/bar, the match can be seen in Figure 13. The blue line, showing cumulative water influx, nicely matches the calculated gas void space replaced by water, shown with the orange boxes. The reservoir pressures and calculated aquifer pressures are also shown with respectively the red and green lines.

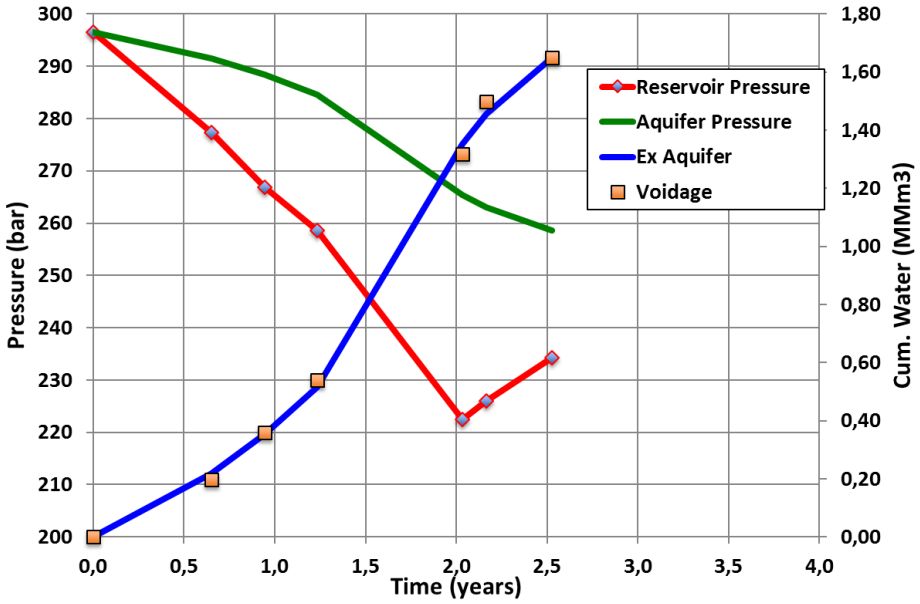

Figure 13. Voidage replacement plot Q16-Maas for Fetkovitch aquifer

3.2.5. Segregated Flow

The Reservoir Saturation Tool (RST) determines hydrocarbon and water saturations behind casing (Schlumberger, 1994). From the RST data collected on the 1st of June a pocket of gas was found below the lowest perforation, in the Upper Detfurth. This was considered to be odd as nearly 50% of the water was coming in from the lowest perforation, see Table 1, and the well log data and the core data did not show any indication of an impermeable layer that could trap the gas. Appendix B shows saturation indications from the RST.

It is assumed that the capillary pressure threshold in the low permeable Lower Hardegsen is the reason for this phenomenon. It was observed that there was no gravity drainage of water from the Middle/Upper Hardegsen to the Upper Detfurth, while the Upper Detfurth water table has risen, and therefore gas had been produced. Water invasion was limited by the introduction of this capillary pressure threshold. A sketch of the expected state of the reservoir is given in Figure 14.

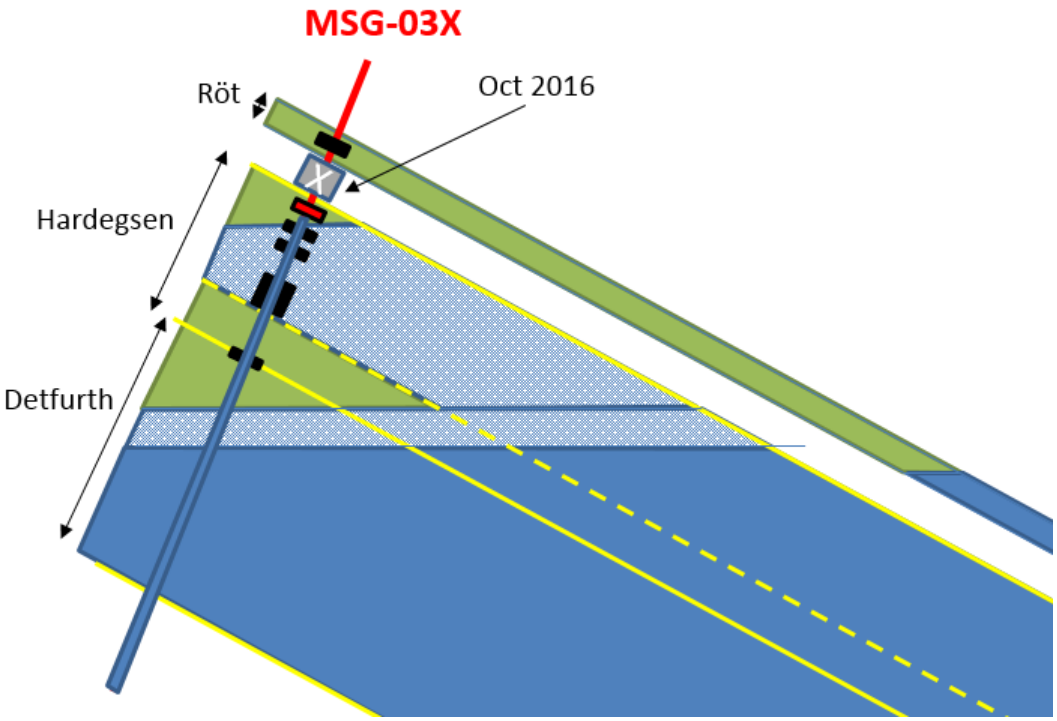

Figure 14. Sketch of expected situation as Hardegsen and Detfurth are plugged off

As the water production wasn't significant at that moment, the Detfurth was perforated together with the lower Hardegsen, as already mentioned in subchapter 3.2.1. The perforated Detfurth soon became less productive due to waterloading from the Hardegsen.

3.2.6. Relative Permeability Curves and Capillary Pressures

The relevance of the relative permeability curves together with the capillary pressure curves have already been emphasized in the previous subchapter. It has been chosen to use different relative permeability curves for different reservoir layers. Each layer's relative permeability curves were calculated with the help of the saturation height function based on well log data.

Table 4 shows the relative permeability parameters for each layer, Appendix C shows the calculated relative permeability curves and Figure 15 shows the capillary pressure curves for each layer.

Layer	Upper Röt	Lower Röt	Upper Hardegsen	Middle Hardegsen	Lower Hardegsen	Upper Detfurth
Threshold Pressure [psi]	3	3	0.5	3	45	3
Sgcr	0.34	0.32	0.15	0.23	0.2	0.26
Ng	2	2	2	2	2	2
Krg'	0.75	0.85	0.9	0.8	0.5	0.8
Swcr	0.3	0.3	0.15	0.4	0.6	0.4
Nw	3	3	3	3	3	3
Krw'	0.2	0.3	0.3	0.3	0.3	0.3

Table 4. Relative permeability parameters per layer

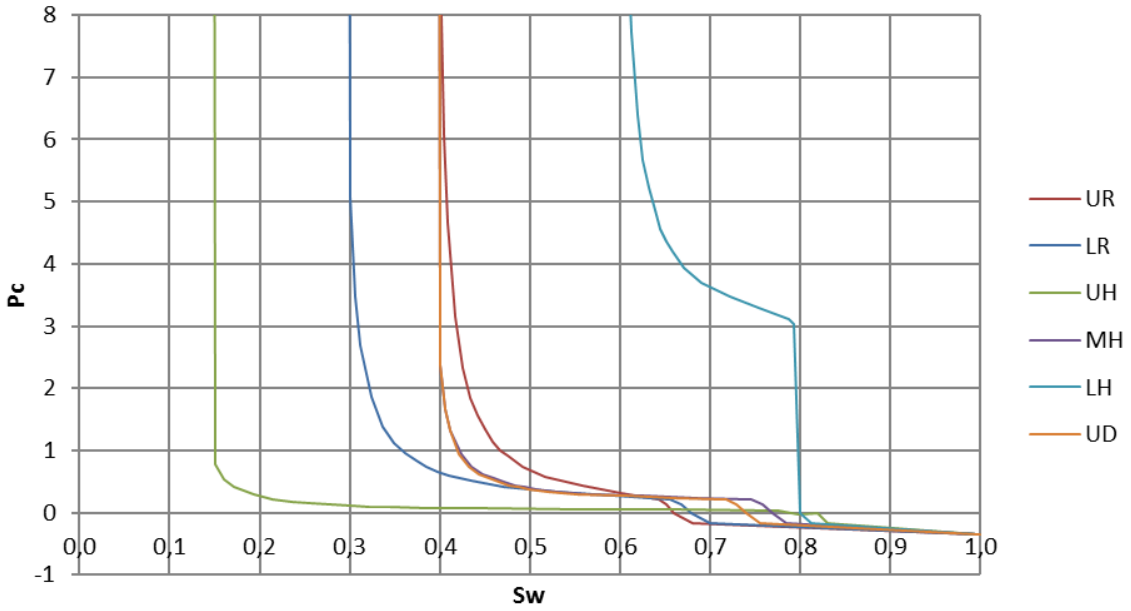

Figure 15. Capillary pressure curves per layer

The capillary pressure curves depicted in Figure 15 show that with increasing porosity, the capillary pressure is lower. As can be seen, the Upper Hardegsen (UH) has the best reservoir quality, i.e. porosity, and has a fitting capillary curve to go with it. Equation 4 below, shows the capillary pressure formula, and its relation to porosity $[r]$.

Equation 4. $$P_c = p_{nw} - p_w = \Delta p = \frac{2\sigma}{r}$$

Previous studies conducted by Oranje-Nassau Energie, had shown that improbable vertical permeability values needed to be applied to the Lower Hardegsen to get a segregated flow like shown in Figure 14. The other option was to have the capillary threshold to be high enough so that no water could pass through. This can be seen in the Lower Hardegsen (LH) in Figure 15.

3.3. Reservoir Fluid

The Q16-Maas reservoir fluid is a retrograde gas-condensate. It has a high specific gravity with more than usual intermediate components and heavy components. Four products are sold: dry gas, propane (C_3H_8), butane (C_4H_{10}) and condensate(C_{5+}). The propane and butane are mixed to a liquid petroleum gas (LPG) blend.

Two RCI (Reservoir Characterization Instrument) samples were used by CoreLab to measure the composition of the reservoir fluid and to derive reservoir fluid properties. The first sample was acquired in the Upper Hardegsen (4723.9m MD) and the second in the Lower Detfurth (4791.6m MD). Next to RCI samples, two DST (Drill Stem Test) samples were analysed. These were obtained by recombining gas and liquid samples from the separator at the measured condensate-gas ratio's (CGR's). Because of the reliability and the fact that it was acquired at monophasic conditions, the Upper Hardegsen RCI sample was considered most reliable and used in the model. Table 5 shows a summarised version of its composition. The table of its exact composition can be found in Appendix D.

Q16-Maas Reservoir Fluid	RCI (4723.9m MD) [mol%]
H_2S	0.00
CO_2	0.54
N_2	2.00
C_1	74.57
C_2	9.18
C_3	4.90
iC_4	1.12
nC_4	1.52
C_5	0.01
iC_5	0.63
nC_5	0.57
C_6	0.75
C_{7+}	4.21

Table 5. Q16-Maas reservoir fluid composition based on MSG-03X RCI sample

A portion of the open hole gas sample was brought back to original downhole conditions, 111.2°C (reservoir temperature). A constant composition expansion (CCE) was then performed during which the dewpoint was determined and retrograde liquid build up was measured until a maximum volume was reached. Pressure-volume data for the single phase and two phase fluid were also obtained. Appendix E shows the measured points and some of these are plotted in Appendix F to show the retrograde liquid curve at constant reservoir temperature. (CoreLab Reservoir Optimization, 2011)

3.4. Conversion to Compositional Model

A history-matched E100 model was provided for this case study. The CO2STORE keyword for E100 in Eclipse, that would also suite this research, cannot be used in combination with the aquifer presence and more intermediate and heavy components. Consequently, this research needs a compositional reservoir simulation model (E300) in order to more accurately simulate the observed reservoir behaviour.

The following changes have been made to the E100 model and are further discussed in the following subchapters:

- Water and Gas phases changed to nine compositions with Peng Robinson Equation of State
- Relative permeability curve for heavier hydrocarbons
- Additional PVT data needs to be added for the 9 components

3.4.1. Nine Components

From a study done by SGS Horizon for this field, a compositional model has already been made, but does not include the recent water production and did not correctly forecast the gas production. SGS Horizon researched the sensitivity of using different components and they concluded that a 9-component composition had the smallest difference and quickest computing time when compared to the fully composition (22 components) model. Table 6 shows the 9 components and the accompanying mole weights.

	Zi [%]	Mol. weight [u]
N_2-C_1	76,57	16,36
CO_2	0,54	44,01
C_2	9,18	30,07
C_3	4,9	44,10
C_4	2,64	58,12
C_5-C_6	2,39	79,08
C_7-C_8	1,8	100,28
C_9-C_{13}	1,33	141,62
C_{14+}	0,65	242,98

Table 6. Components for E300 reservoir model

3.4.2. Oil Relative Permeability

The original history matched E100 model only had water and gas components and thus only water and gas relative permeability curves. As the compositional model includes heavier 'oil' (or condensate) components, a new set of relative permeability curves are needed. The SOF3 function in Eclipse is a three-phase oil saturation function. It plots the oil saturation against the corresponding oil relative permeability for regions where oil and water are present, and another where oil and gas are present. It is vital for the simulating of a veracious reservoir as the condensate blockage strongly depends on this. The oil-water relative permeability curve is considered to be the same as the oil-gas relation, except for first set of curves taken from the Eclipse manual as can be seen in Figure 16. Three different SOF3 functions are used in the simulations and shown in Figure 16.

- The first is taken directly from the Eclipse Technical Manual. This SOF3 function is made for oil reservoirs and thus is probably not a good indication for the condensate that comes from retrograde gasses. [SOF3]
- The second is taken from a radial study done in a Wet-gas radial box model that was used to test condensate blockage in E100. [RAD]
- The third is a fit-for-purpose SOF3 function that transitions the history-matched gas production from the Röt to the forecasted gas production very nicely. It was made using trial-and-error to fit the production profile to transition smoothly. [SOF3_NEW]

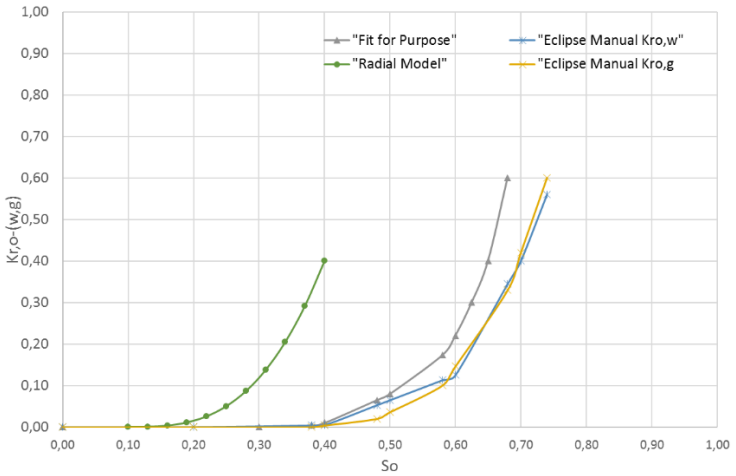

Figure 16. SOF3 curves for tested scenarios

The oil relative permeability curves are the same in each layer. The results of the different production profiles are shown in section 3.5. The oil relative permeability curves can be considered to be pseudo-curves, as the effects of condensate blockage are considered to occur on a smaller scale than the actual grid block size.

3.4.3. PVT Data

From the same compositional model from SGS Horizon study, the PVT Data can be taken. It was created in PVTsim, which is not available at Delft University so unfortunately the exact manner in which the PVT was built is unavailable. However, PVTi, which is supported by Eclipse, can be used to show the compositions phase diagram. There is an unwanted outlier in the data because there is a transition in the PVTsim and PVTi programme. This does not impact the model as this outlier is a point for the static separator conditions and does not influence the downhole behaviour of the reservoir fluid. Figure 17 shows the phase envelope that is taken from the Xodus Reserve Audit report (Xodus Advisory, 2016).

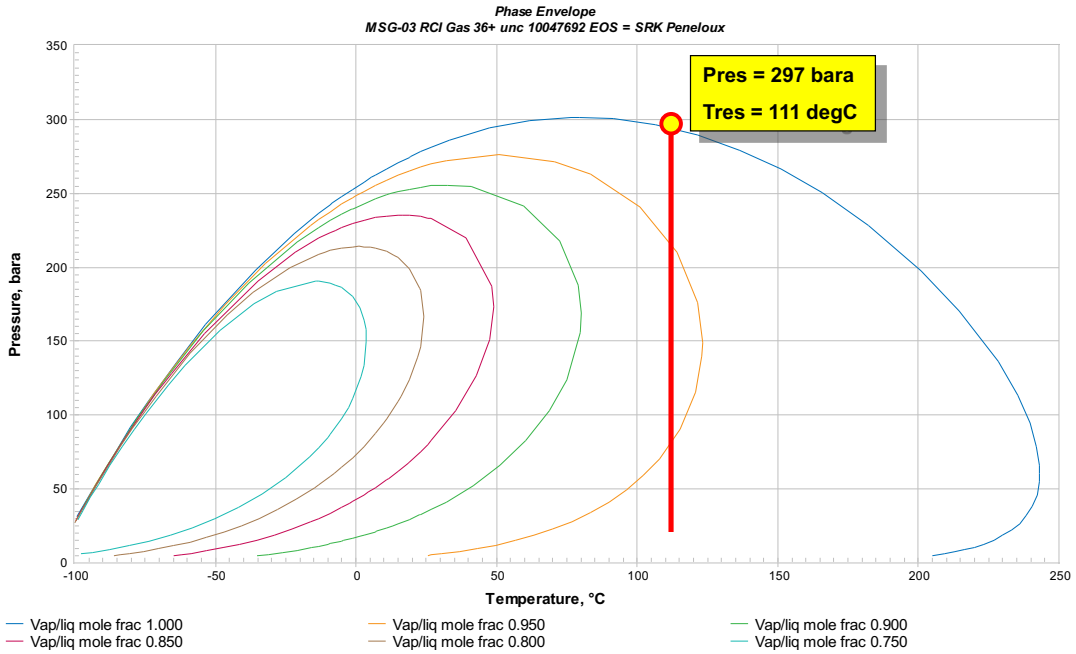

Figure 17. Phase envelope of Q16-Maas reservoir fluid; (Xodus Advisory, 2016)

3.5. History Match Results

The reservoir simulation is history matched until the 1st of January 2017. This was roughly the starting date of this case study and has been chosen not to update as time progressed to ensure continuity and not have to constantly update the production profile. The current situation can be used as an indication to check the forecast is working as it should.

With the model being converted from E100 to E300, a completely different property evaluation is used that gives a higher gas initially in place (GIIP). Just to evaluate this impact of converting E100 to E300, the blackoil E100 history match has been run in E300. This caused converging issues, but did show a clear increase in GIIP. The GIIP for the E100 is 1.14E9 sm^3 compared to 1.22E9 sm^3 for E300, giving an increase of roughly 7%.

When comparing the water production for the E100 model and the compositional E300 model, one can see that the water production history is not matched for the E300 case. By reducing the total pore volume of the reservoir one can force the water breakthrough to happen earlier and thus history match better with the known water production. As the total volume of the reservoir is still

uncertain, because the P/Z is influenced by water influx from the aquifer, three different pore volumes have been chosen to be part of the sensitivity of this research.

- The first pore volume is the original pore volume that the E300 reservoir has.
- The second is the exact ratio of GIIP change due to the conversion from E100 to E300, a pore factor reduction of 0.96.
- The third pore volume reduction is the ratio of the E100 history matched black oil model was run in E300 and has a rounded-off pore reduction factor of 0.93.

If three pore volume cases are considered and three oil relative permeability curses are possible, nine different cases present themselves.

In Figure 18 the gas and water production rates for all three pore volume cases are shown from the 1st of January 2016 until the 1st of January 2017. The relative permeability curves that are fit-for purpose, mentioned in subchapter 3.4.2, are used in each case. The main difference is in the water production and the 0.93 pore volume reduction reservoir has the best match to actual data, plotted with crosses.

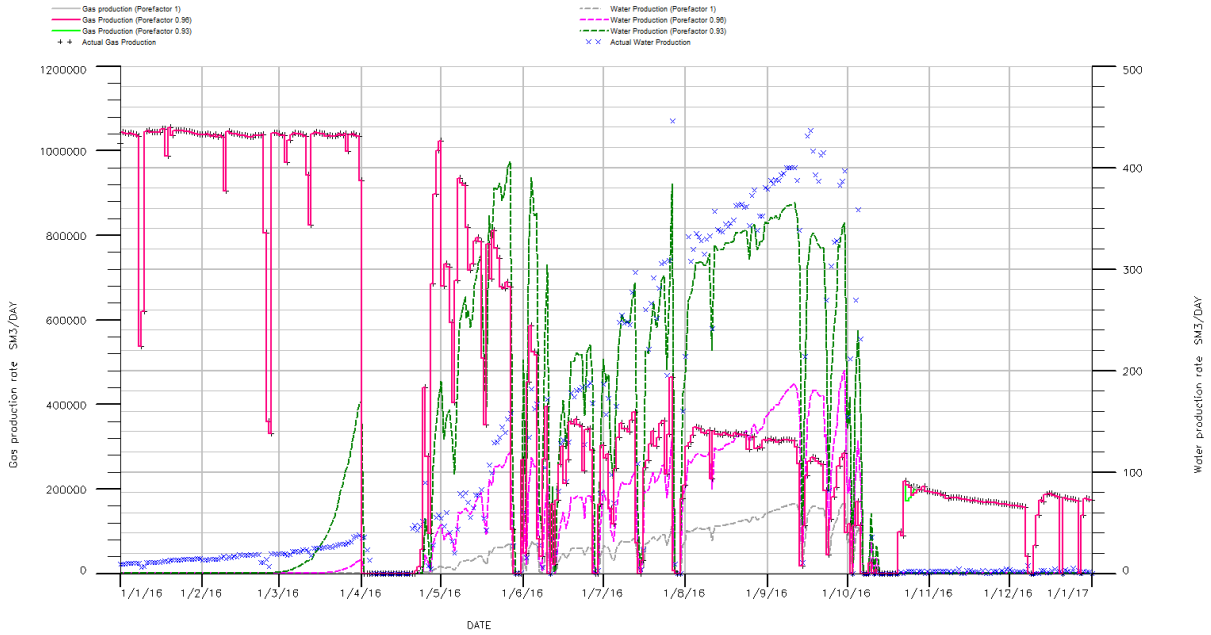

Figure 18. Gas and water production rates for SOF3_NEW relative permeability curves, with actual production data

Also, a cross section of the reservoir should show a resemblance of the expected sketch as in Figure 14. Figure 19 shows a cross section of the initial molar density (moles per cubic meter) of the reservoir for the 0.93 pore factor and the fit-for-purpose relative permeability. Figure 20 shows the same molar density cross-section for the 1st of January 2017, the end of the history match.

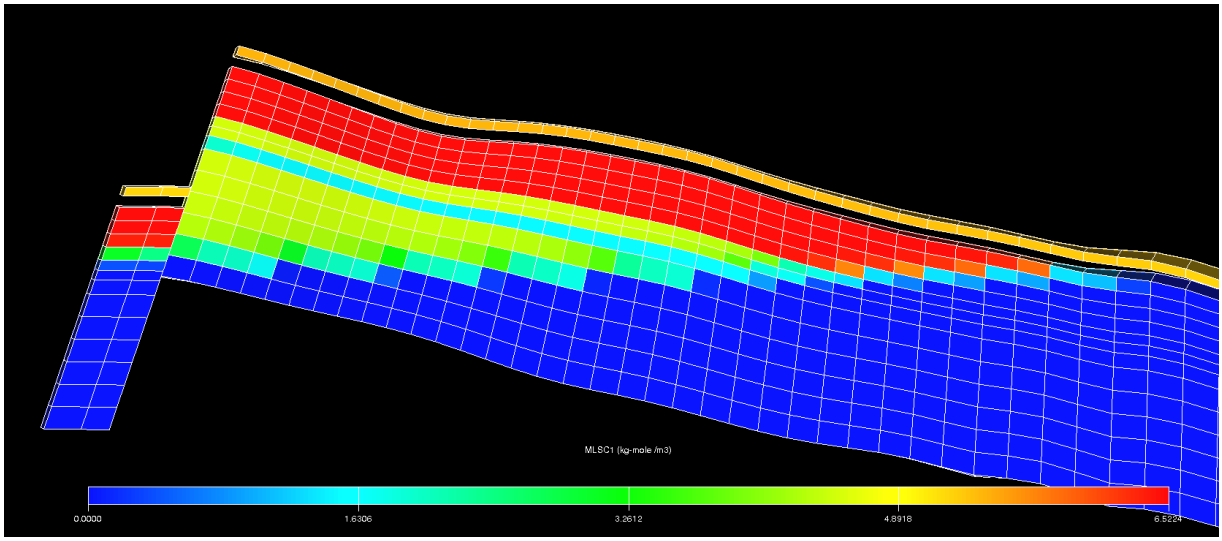

Figure 19. Reservoir cross-section showing molar density at 1st of April 2014 (z-direction enhanced x2)

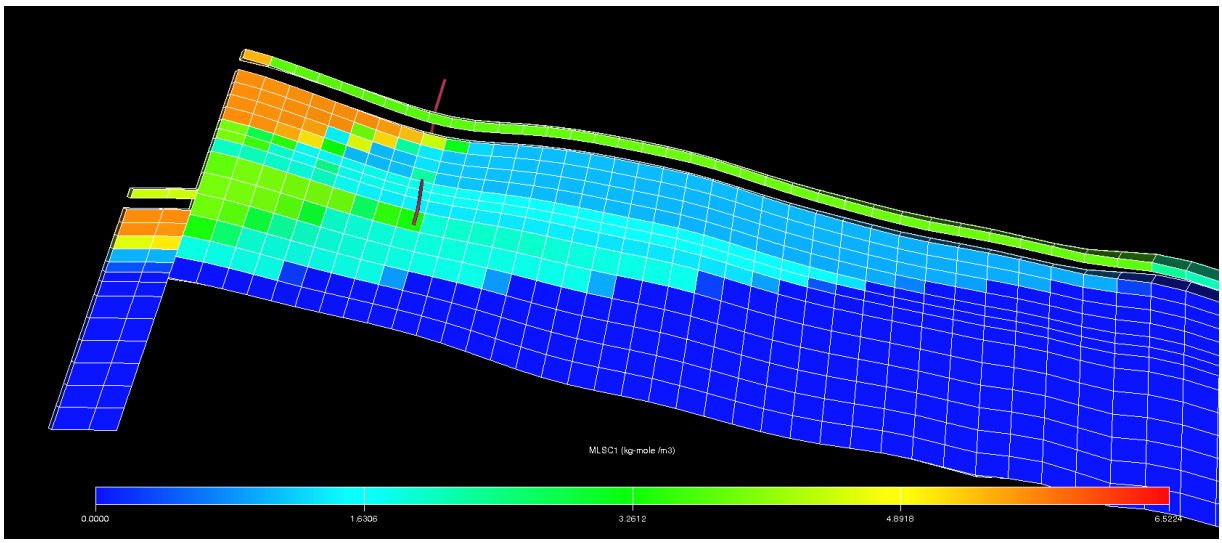

Figure 20. Reservoir cross-section showing molar density at 1st of January 2017 (z-direction enhanced x2)

Figure 20 shows the gas component density after roughly 2.5 years of production. The gas molar density significantly declines over time showing results of production. Water has encroached from the aquifer below and is replacing the void space left by the gas.

When comparing Figure 20 with Figure 14, the expected sketch, there is very strong resemblance. The preliminary water breakthrough is through the Hardegsen and a gas volume remains in the Detfurth as the intruded water from the Hardegsen does not segregate due to the entry pressure of the lower Hardegsen.

As can been seen in Figure 20, a significant amount of gas remains in the attic of the field. Chapter 4, Field Life Extension, studies the possibility of recovering this remaining attic gas.

4. Field Life Extension

In the previous chapter, a significant amount of untapped gas and condensate is shown to remain in the attic of the reservoir. The history matched production profile from the previous chapter, can now be used to forecast future production strategies. In this chapter, the forecast models are shown and discussed, and the potential for field life extension by means of a sidetrack are simulated. The consequences of producing the remain gas on CO_2 storage is shown in chapter 5.

4.1. Forecast

By continuing with the simulation after the history match, a forecast for future production can be predicted. For this case study nine models were produced, 3 variables for pore volume and 3 variables for relative permeability curves. For all nine models, the forecasts are run until the well is shut due to operational restrictions. The constraints are either a minimum gas production rate of 65000sm^3/day or a water gas ratio larger than 1,1E-3sm^3/sm^3. The water gas ratio constraint is set to make sure the water doesn't kill the well and is based on the maximum water cut that was possible pre-Hardegsen plugging. The minimum gas production rate is the lowest rate operationally possible.

The history match of the relative permeability curve taken from the radial model (RAD) already showed that there was a minimal Röt production and the same trend can be noticed when forecasting, see Appendix G. A large increase in production can be seen as the forecast commences for the eclipse manual (SOF3) relative permeability curve. This shows that the relative permeability curve taken from the manual, was constrained by actual production. The fit-for-purpose (SOF3_NEW) relative permeability curves, as the name suggests, shows a nice transition from history match to forecast.

When an overview of the field is taken after the production was stopped, all cases show remaining gas up dip in the structure. This shows potential for attic gas recovery, either by means of a sidetrack or a new well. As a sidetrack is cheaper, this will be considered the preferred alternative for further field life extension. Table 7 shows the remaining gas volumes in the main reservoir and Figure 21 shows the location of the gas pocket within the reservoir.

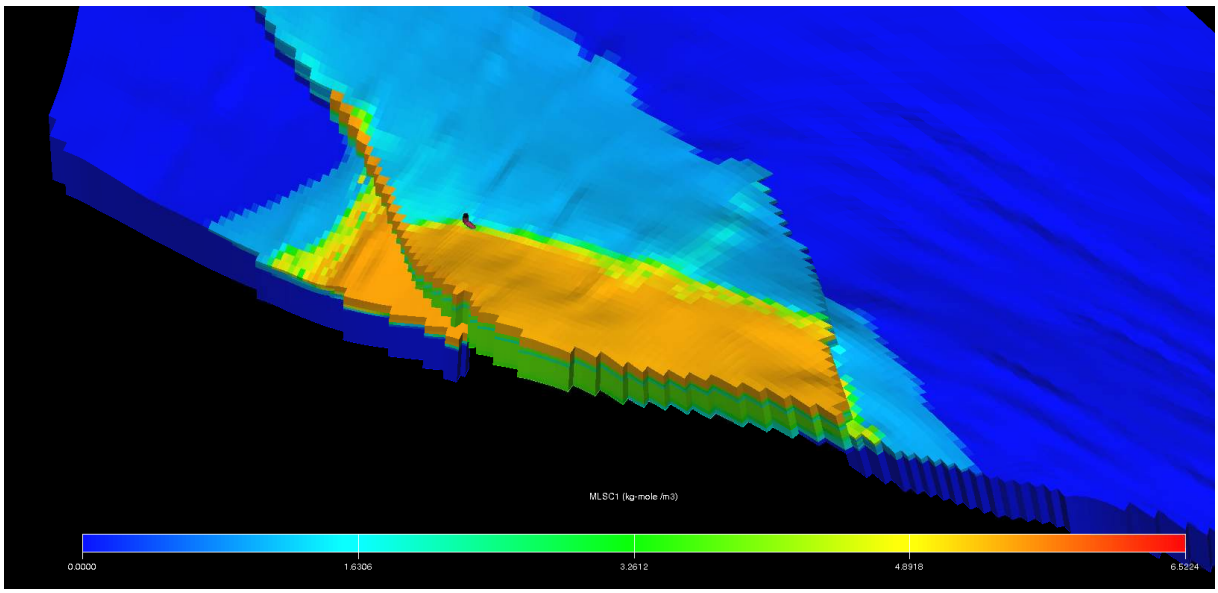

Figure 21. Molar density of component 1[N_2-C_1H_4] after history match, showing remaining gas pocket in Hardegsen

Layer	Remaining volume [sm^3]
Lower Röt	3,58E+07
Upper Hardegsen	2,44E+08
Middle Hardegsen	5,48E+07
Lower Hardegsen	2,18E+07
Upper Detfurth	1,70E+08

Table 7. Remaining gas volume per layer

4.2. Sidetrack Location

The initial well location of MSG-03X was planned without taking into account the aquifer presence. The location of MSG-03X is downdip, leaving valuable untapped gas condensate trapped in the 'attic' of the reservoir. The location of the proposed sidetrack is considered such that it passes though the Röt, Hardegsen and Detfurth in an updip location, 17 meters higher, compared to the MSG-03X well. To ensure the sealing potential of the northern fault is not compromised a distance of at least 50m from this fault is to be maintained. The proposed sidetrack location is shown in Figure 22.

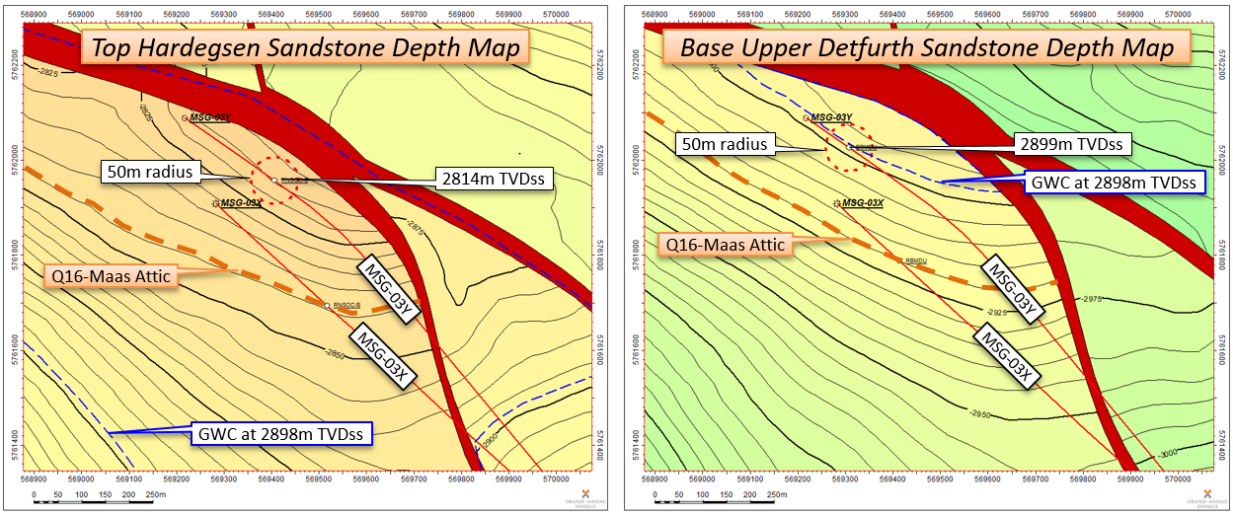

Figure 22. Sidetrack (MSG-03Y) planned well trajectory (left: Top map Upper Hardegsen, right: Base map Upper Detfurth)

4.3. Attic Gas Production

The proposed production strategy for the sidetrack, is to first produce the Röt and Detfurth together, and after an operational limitation is reached, then to produce the Hardegsen. This strategy is chosen to defer production from the Hardegsen where significant water production was observed from the original MSG-03X well.

The same operational constraints that were set for the final stages of the original well production were also set for the sidetrack production: minimum gas production rate of 65000sm^3/day or a water gas ratio of no larger than 1,1E-3sm^3/sm^3. The additional production results can be found in Table 8.

Pore	Rel Perm	Röt+Detfurth [sm^3]	Hardegsen [sm^3]	Gas production [sm^3]	Additional production [%]	Water production [sm^3]	Röt+Det Shut Down	Hard Shut Down
0.93	SOF3_NEW	5.18E+07	1.14E+08	1.66E+08	26.3%	8.40E+03	Gas	WGR
0.93	SOF3	8.36E+07	9.93E+07	1.83E+08	30.2%	1.68E+04	WGR	WGR
0.93	RAD	6.16E+07	1.01E+08	1.62E+08	25.3%	1.51E+04	WGR	WGR
0.96	SOF3_NEW	6.26E+07	1.29E+08	1.92E+08	30.4%	9.96E+03	Gas	WGR
0.96	SOF3	9.99E+07	1.14E+08	2.14E+08	35.3%	1.74E+04	WGR	WGR
0.96	RAD	7.49E+07	1.13E+08	1.88E+08	29.1%	1.48E+04	WGR	WGR
1	SOF3_NEW	7.50E+07	1.46E+08	2.21E+08	34.8%	1.32E+04	WGR	WGR
1	SOF3	1.15E+08	1.30E+08	2.45E+08	40.6%	1.71E+04	WGR	WGR
1	RAD	8.82E+07	1.27E+08	2.15E+08	33.2%	1.62E+04	WGR	WGR

Table 8. Additional sidetrack production data for all scenarios

The results in the table show that a significant amount of gas can still be produced with the sidetrack, for all scenarios. The additional production percentage in column 6, shows the percentage of production that is recovered additionally, compared to the total production before sidetracking. The reason for the well shutting down is given in the last two columns and can either be the gas limit (Gas) or the water-gas ratio limit (WGR). The production results for all cases, can be found in Appendix G. In the results section 7.2.1, the additional benefit from the sidetrack is calculated.

5. CO_2 Injection

The two previous chapters offered two scenarios after which CO_2 can be injected. This chapter covers the CO_2 storage potential of the Q16-Maas field. The production strategies show different storage volumes and going with a sidetrack option and extending field life is advantageous not only for added profit from gas sales, but also increases storage volume.

5.1. CO_2 Injection into Q16-Maas

The great benefit of storing CO_2 in the Q16-Maas field is the fact that the logistical costs for this project are low compared to other offshore fields. Due to its onshore facility and the strategic location, close the port of Rotterdam and the CO_2 supplier, it dramatically reduces transportation costs. For offshore fields, the additional costs for CO_2 transport through pipelines rapidly becomes uneconomical at current ETS prices. This is due to the fact that CO_2 forms carbonic acid that is corrosive. CO_2 pipelines are therefore designed to be corrosion resistant, often using chrome alloy, that is 10% more expensive than regular L80 steel pipe commonly used for gas pipelines of similar size and length (Essandoh-Yeddu & Gülen, 2009).

Also, any retrofitting of CO_2 service equipment at the surface- or wellsite is cheaper in the case of onshore CO_2 injection as compared to offshore modification costs.

Initially, when the ROAD project was initiated, a field further offshore in the P18 concession block was considered for CO_2 storage. Although the field is larger and it would have more CO_2 storage capacity, the costs would be prohibitively high for a pilot project. The following chapter looks into the potential CO_2 storage volume and also considers the possibility of storing CO_2 above the initial reservoir pressure as this directly affects the amount of storable carbon dioxide. CO_2 storage can only start in 2020, as all the facilities for the capturing and injection need time to design, fabricate and install, so this is considered the starting date for all injection scenarios.

A limit of 290 bar for the bottomhole pressure (BHP) is set to ensure the reservoir containment properties are not compromised as this pressure is slightly lower than the initial reservoir pressure. An injection rate of just over 2 million sm^3/day (calendar day) is assumed and the downtime is considered to be 1/3 of the total injection time. Eclipse directly considers this downtime and this gives an injection rate of roughly 1.3 million sm^3/day (injection day). The 2 million sm^3/day injection rate is considered as this was necessary for the field to store 2 million tonnes of CO_2 over 2 years, with the downtime, as this was the ROAD project's initial goal. This injection quantity is also based on the expected CO_2 capture rate of the neighbouring coal-fired power plant.

5.2. Without Sidetrack

There is a direct link between the initial pressure at which injection starts and the amount of potentially storable CO_2, as can be seen when comparing the same scenarios in Table 9 and Table 10. This is because the initial CO_2 injection pressure depends on reservoir pressure at that time. The reservoir pressure, in turn, depends on the volume of fluids recovered from the field compensated with the aquifer fluid influx. Without the sidetrack production the pressure is higher when injection commences. This consequently means that less CO_2 can be stored. Table 9 shows the total production until injection starts, the total injection in sm^3 and in million tonnes. A CO_2 density of 1.842kg/m^3 is used. Also, what is interesting to note, is the bottomhole pressure that exists as injection starts which can be found in the 2nd column from the right.

Pore	Rel Perm	Total Production [sm^3]	Total Injection [sm^3]	= [MMtonne]	BHP start injection [bar]	BHP limit date
0.93	SOF3_NEW	6.30E+08	5.66E+08	1.04	255.02	6/1/2020
0.93	SOF3	6.07E+08	5.66E+08	1.04	257.00	5/18/2020
0.93	RAD	6.42E+08	5.67E+08	1.04	254.08	6/8/2020
0.96	SOF3_NEW	6.33E+08	5.68E+08	1.05	255.77	6/3/2020
0.96	SOF3	6.06E+08	5.69E+08	1.05	257.98	5/20/2020
0.96	RAD	6.45E+08	5.69E+08	1.05	254.78	6/12/2020
1	SOF3_NEW	6.36E+08	5.70E+08	1.05	256.11	6/7/2020
1	SOF3	6.04E+08	5.70E+08	1.05	258.62	5/21/2020
1	RAD	6.48E+08	5.71E+08	1.05	255.08	6/14/2020

Table 9. Production and injection data for no sidetrack (MSG-03X) forecast

Appendix H shows the production and injection data together with the pressure in the bottom of the hole. What can be seen is that the aquifer brings back the reservoir pressure to approximately the same level for all the cases. This is the reason why there's hardly any difference in the total injectable volume of CO_2. The last column in Table 9 shows the date for which the bottomhole pressure limit of 290 bar is reached. As can be seen in the graphs in Appendix H, at this date, the injection rate that is set can't be maintained as this would increase the bottom hole above the set limit. Consequently, the injection rate is decreased. This limits the injection total.

5.3. With Sidetrack

The same link between initial pressure at injection and storable CO_2 can be noticed for the sidetrack injection profiles in Appendix G. Table 10 shows the summary for the sidetrack production and injection totals.

Pore	Rel Perm	Total Injection [sm^3]	= [MMtonne]	BHP start injection [bar]	BHP limit date
0.93	SOF3_NEW	7.38E+08	1.36	237.22	10/7/2020
0.93	SOF3	7.35E+08	1.35	236.83	10/5/2020
0.93	RAD	7.47E+08	1.38	236.48	10/16/2020
0.96	SOF3_NEW	7.58E+08	1.40	234.55	10/30/2020
0.96	SOF3	7.55E+08	1.39	233.28	11/1/2020
0.96	RAD	7.65E+08	1.41	235.00	11/5/2020
1	SOF3_NEW	7.83E+08	1.44	229.84	12/1/2020
1	SOF3	7.73E+08	1.42	227.45	11/25/2020
1	RAD	7.88E+08	1.45	233.11	12/3/2020

Table 10. Injection data for sidetrack (MSG-03Y) forecast

For this case, the initial bottomhole pressure differs far more than in the non-sidetrack cases. This heavily influences the total amount of CO_2 that is injected as it postpones the reaching of the BHP constraint and consequently limits the injection rate. On average, roughly 350.000 tonnes more CO_2 can be injected if the sidetrack is drilled and used to inject CO_2. This additional injection volume is thanks to the, on average, 22 bar lower bottomhole pressure at which injection starts. The added pore volume does increase injection total slightly, but not as significant as the BHP limit, as can be seen when comparing Table 9 and Table 10.

5.4. Bottomhole Pressure Limitation

By increasing the BHP limit, the maximum injection plateau rate can be maintained for a longer time and thus, more CO_2 can be injected in the same amount of time. This does, of course, come with the drawback that the integrity of the reservoir cannot be guaranteed. Next to the cap rock integrity, the faults are also potentially leak-prone. The closest fault and thus the most hazardous leaking location is still at least 50 meter from the well.

Two new BHP limits have been set, namely, 310 Bar and 330 Bar. They have been implemented for the 0.93 pore factor and fit-for-purpose relative permeability curve scenario as this had the best production match to the actual situation. The injection results are shown in the Table 11 and Figure 23 below. The maximum pressure at the closest gridblock to the fault is also investigated and does not exceed the borehole limit set.

Pore	Rel Perm	BHP limit [bar]	Injection 2y [sm^3]	= [MMtonne]	BHP limit reached	Injection 4y [sm^3]	=[MMtonne]
0,93	SOF3_NEW	290	7,38E+08	1,36	7-10-2020	9,25E+08	1,70
0,93	SOF3_NEW	310	9,48E+08	1,75	6-7-2021	1,28E+09	2,35
0,93	SOF3_NEW	330	1,01E+09	1,87	10-5-2022	1,61E+09	2,97

Table 11. BHP limit variation results

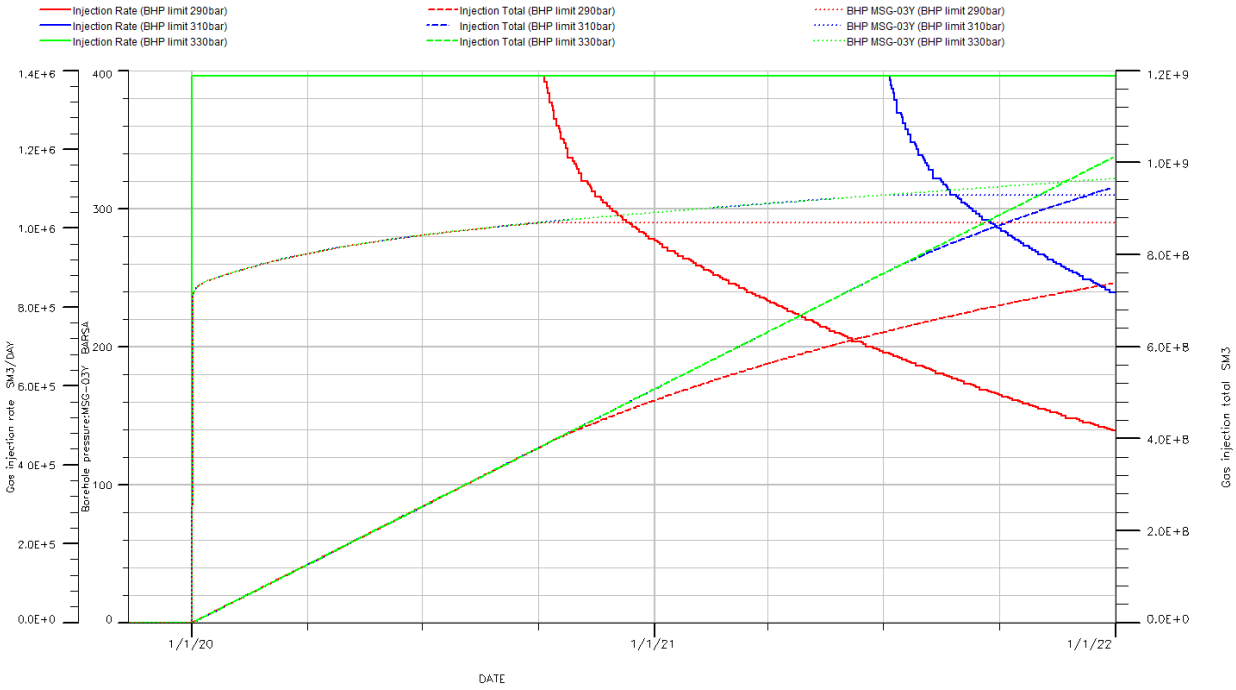

Figure 23. Two year CO_2 injection forecast for different BHP limits

Table 11 shows a significant increase in total CO_2 injection. The injection plateau is maintained throughout the full duration of the simulation for the 330 BHP limit case. If we were to extend the duration by two more years, the moment for which the 330 BHP injection plateau cannot be maintained can be found. The additional injected volume during that period for all 3 limits is shown in Table 11 and Figure 24.

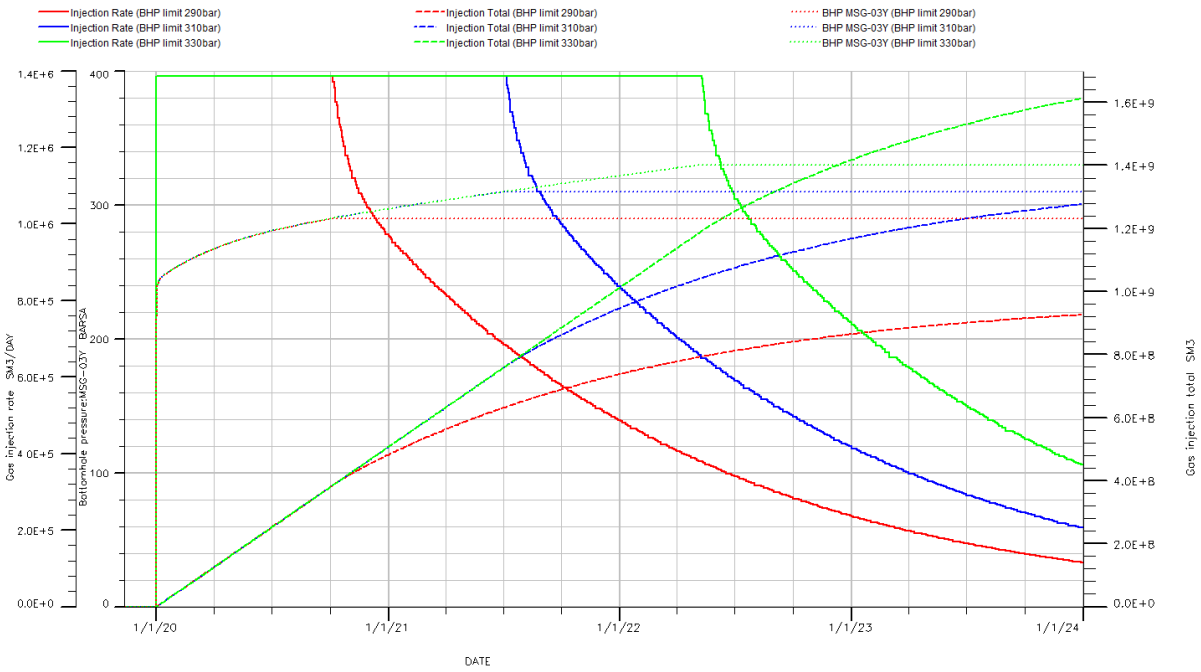

Figure 24. Four year CO_2 injection forecast for different BHP limits

5.5. Aquifer Recharge

To illustrate the recharging of the reservoir due to the water influx, the simulation has been run until January 1st 2022, for both the sidetrack and the original well cases. The resulting average reservoir pressure over time is shown in Figure 25. What can be noticed is that, although the aquifer is large, it is not considered to be an 'infinite acting aquifer' as this would result in the pressure recharging to initial reservoir pressures. Both cases show the pressure reaching different equilibriums after a certain amount of time. The sidetrack average pressure, shown with the green line, has a lower equilibrium pressure than that of the original well, shown with the red line. The fact that the aquifer is not infinitely acting leaves a pressure depletion that can be utilised for CO_2 storage under safe conditions.

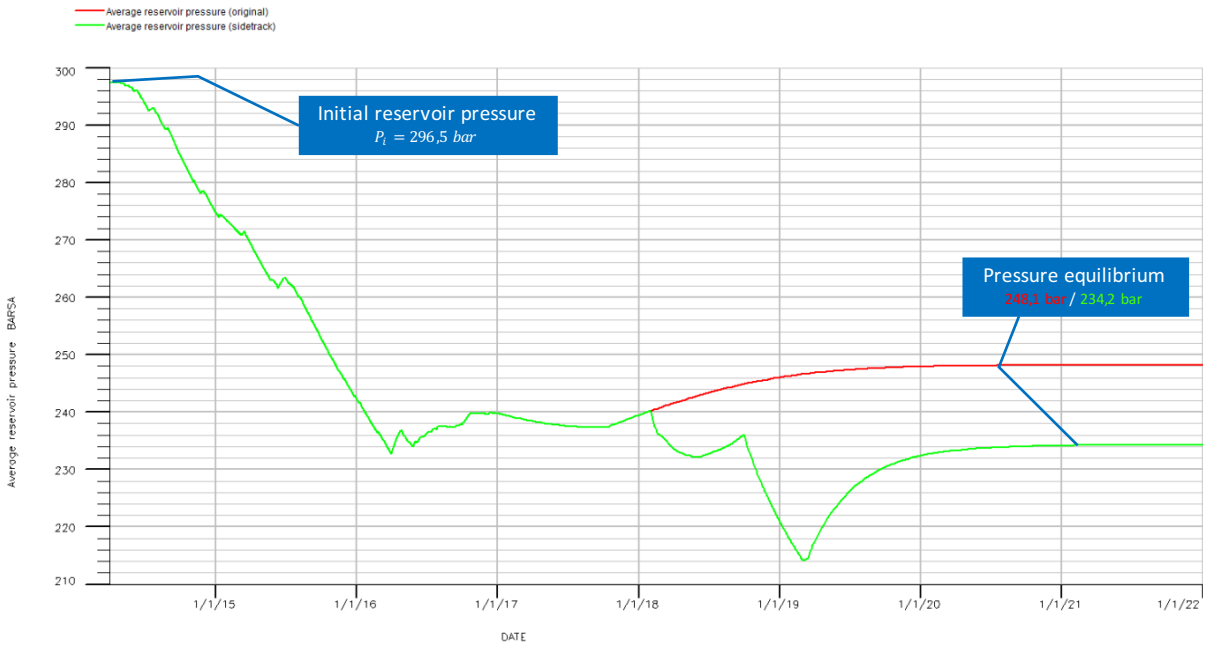

Figure 25. Average field pressures, showing aquifer recharge

6. Enhanced Hydrocarbon Recovery

It was already mentioned previously that the sidetrack could also be drilled as a completely new well, thus presenting the option of injecting and producing at the same time. The injected CO_2 could potentially sweep the remaining gas or help mobilize condensate. This chapter researches the field's potential for enhanced hydrocarbon recovery by means of CO_2 injection.

6.1. Production and Injection Strategies

Separating CO_2 from natural gas is an expensive process. For this study, producing more than 5% CO_2 from the reservoir is not considered a viable option, as this would require separation of the different gasses. Producing more than 5% CO_2 would mean that the injected carbon dioxide is being reproduced as the field naturally contains 0.54% CO_2, see Table 5 and Table 6.

As was previously mentioned, CO_2 injection is only possible as of January 2020. For this chapter, the CO_2 is assumed to be readily available earlier to facilitate enhanced hydrocarbon recovery.

The remaining volumes of gas in the formations, shown in Table 7, still apply for this case. The 0.93 pore factor and fit for purpose relative permeability curves simulation provides the best history match and is therefore the case that was used to simulate the effect of CO_2 injection and enhanced hydrocarbon recovery.

6.2. Sweep Hardegsen

By tactically injecting CO_2 ahead of the aquifer water intrusion, could the sweep be better than the natural water sweep from the aquifer? The scenario assumes that CO_2 is injected at just over 20000 sm^3/day (calendar day) at the same time as the Hardegsen is produced. Significant condensate blockage is unlikely because the reservoir quality of the Hardegsen is good, so mobilizing oil is not expected. The objective of simulating the CO_2 injection into the Hardegsen is to investigate whether a more efficient sweep can be realized. Figure 26 shows the results.

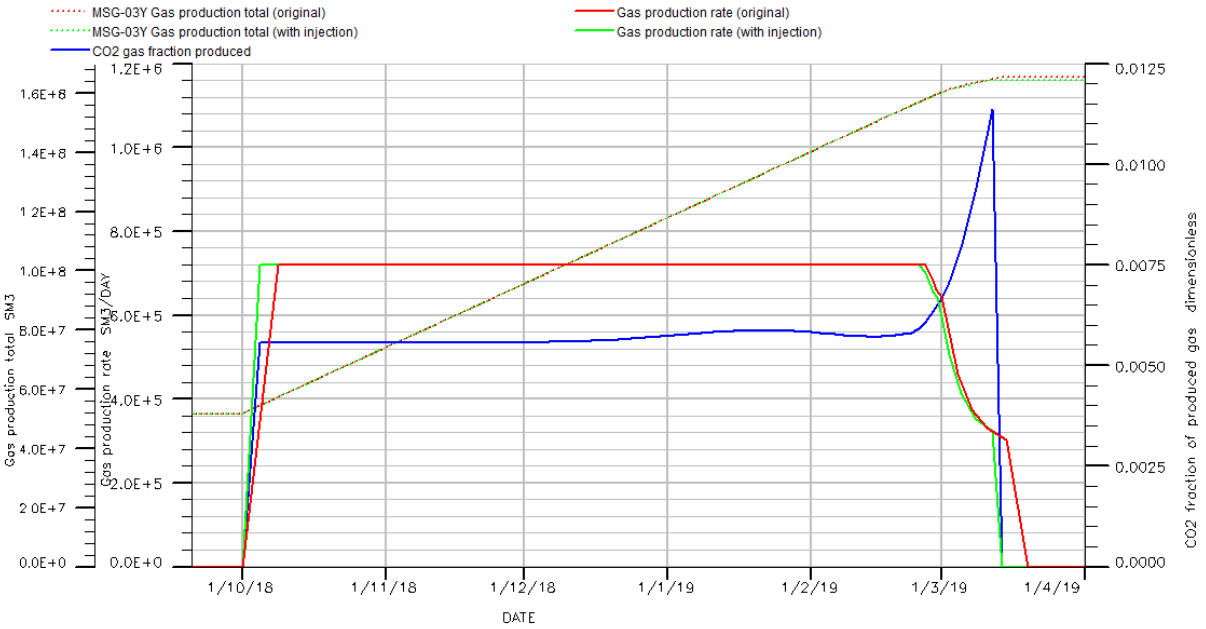

Figure 26. Gas production and total of Hardegsen sweep strategy

The simulation run shows that there is a very sharp increase in CO_2 in the produced gas, representing CO_2-breakthrough. The reason for shut-in is that the water-gas ratio limit is reached. This scenario actually shows negligible difference in cumulative production compared to the original scenario without CO_2 injection. The Hardegsen layer is already swept so efficiently by the water from the aquifer that any attempt to produce more from the Hardegsen by injecting CO_2, is restricted by the CO_2 breakthrough.

The total CO_2 storage volume that can be injected after commingled production and injection is also lower, primarily because the original well (MSG-03X) is used. Due to the additional hydrostatic pressure in the deeper part of the reservoir, the pressure is higher when injection commences. As previously mentioned, there is a direct correlation between BHP at the start of CO_2 injection and total amount of storable CO_2.

6.3. Mobilize Residual Condensate in Röt

The Hardegsen layer's good reservoir quality restricted any commingled strategy for CO_2 injection and additional gas production. The Röt however is of far lesser reservoir quality and could hold a significant amount of immobile condensate. In the simulation run, CO_2 is injected at just over 20000 sm^3/day (calendar day), which is 1/100th of the CO_2 injection rate assumed for storage (chapter 5). The injection starts together with the start of production from the Röt and the Detfurth. Figure 27 shows the production profile of the Röt and the Detfurth.

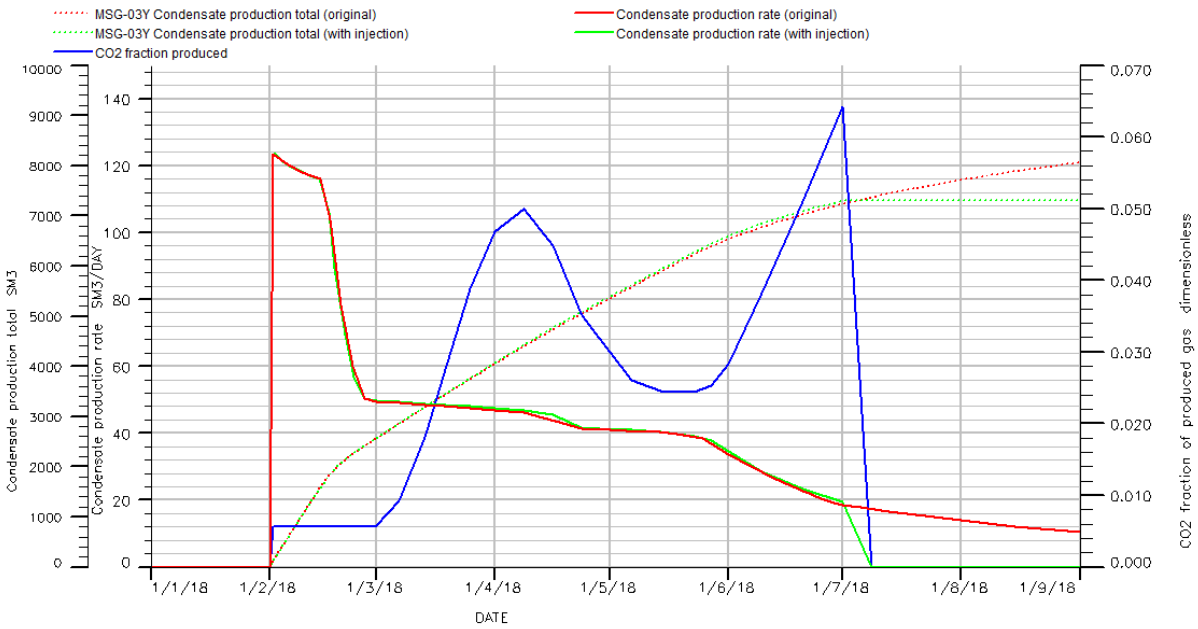

Figure 27. Condensate production rate and total from Röt and Detfurth formations

Less condensate is produced when injecting into the Röt and producing from both the Röt and the Detfurth. As can be seen in Table 7, there is only a limited volume of gas remaining in the Röt. The keyword restriction for the CO_2 that is used in the simulation restricts the gas inflow of the Röt and causes the dip in CO_2 production from just after April till mid-May. After the majority of gas is produced from the Detfurth, the Röt is reopened and a quick CO_2 impulse can be seen in July. If focus is purely on the extraction of condensate from the Röt the following production profile can be seen, see Figure 28. Again, this is as CO_2 is injected right from the start.

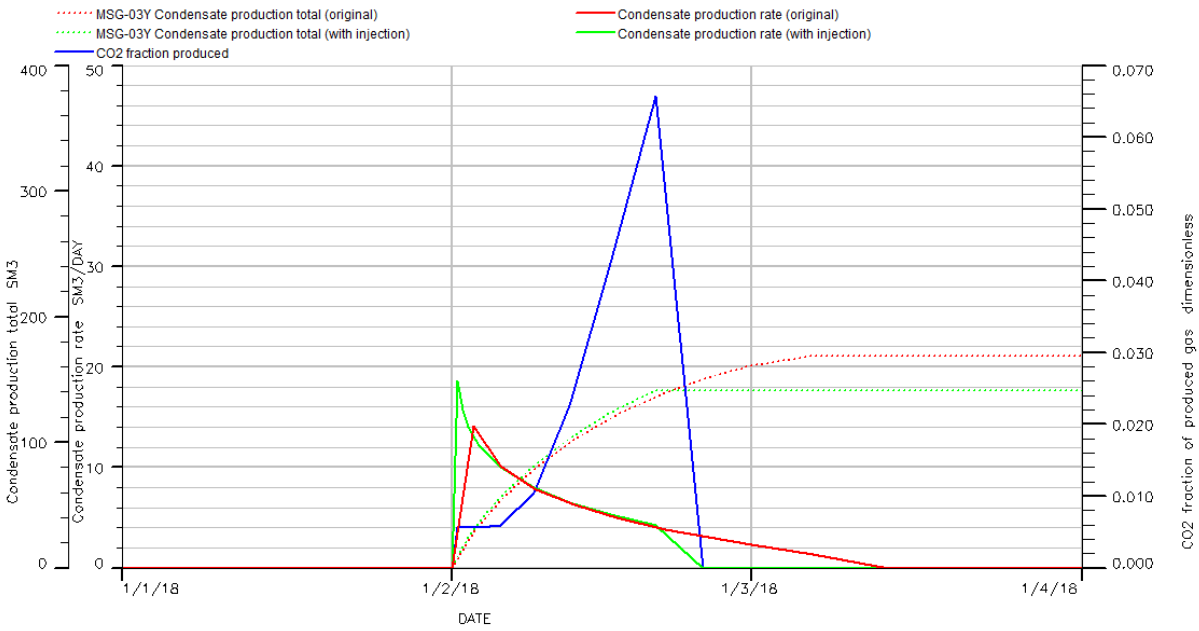

Figure 28. Condensate production rate and total from Röt formation

As production drops due to the production of CO_2, a similar production strategy was applied, but now CO_2 is injected 2 weeks into the Röt production and is injected at 5 times the rate. This did not show any promising results as the BHP limit was reached very quickly, causing the injection rate to be brought down. The gas production limit was even reached earlier because of the smaller iteration steps taken by the simulator to cope with the injected CO_2 calculations.

The fact that this formation is thin, with a thickness of only 3.6 meters, probably contributes to the fact that no real injection strategy works as the CO_2 shoots through the formation and quickly causes the gas production in the well to reach the maximum CO_2 production rate.

6.4. Discussion

The goal of enhanced hydrocarbon recovery for this field was to simulate and test two things. First, the sweep of the water may be improved by injecting CO_2 ahead of the waterfront (coming from the aquifer influx). Second, immobilized condensate that dropped out in the Röt may be respressurized, consequently becoming more mobile and leading to increased condensate production.

The injecting of CO_2 ahead of the water did not show any significant increase in production. When examining Figure 20, the water front shows a high angle of intrusion, showing a stable Dietz gravity-segregated displacement. This brings the conclusion that the sweep of the water can be considered to be very effective and injecting CO_2 for the purpose of enhancing recovery is unprofitable.

For repressurizing and mobilizing valuable condensate in the Röt formation, the injection of CO_2 seemed to be viable. The sheer thickness of the layer however impedes any such enhanced oil recovery. The injected CO_2 is quickly recovered through the production well, that consequently will lead to unwanted and expensive separation processes.

It should be noted that reservoir simulation provides a non-unique solution to simulate reservoir performance because of multiple assumptions when upscaling from core data and well data to reservoir data. Likewise, the accurate simulation of CO_2 injection to boost production is inherently uncertain.

7. Cost Analysis and Economics

In this chapter, the additional costs of storing CO_2 are reviewed. The cost for a sidetrack well and gas sales potential are calculated. The transport of CO_2 from the power plants to the field, the extra surface facilities needed and the downhole completion changes are discussed. The European Union Emissions Trading System is considered and a break-even-point for this particular storage project will be calculated considering transport and storage only.

7.1. Costs Analysis

7.1.1. Transport Costs

For the transport of CO_2 from the power plant to the Q16-Maas facility an onshore high pressure pipeline is needed together with a high-pressure CO_2 compressor. The estimated costs are respectively €15M and €10M-€15M, bringing the total to €25M-€30M for the high-pressure CO_2 facilities.

The Port of Rotterdam is looking to become a CO_2 hub to meet climate targets from the industry and attract new low carbon business to the port. Rotterdam already has a CO_2 pipeline operated by OCAP. This joint venture supplies greenhouses with CO_2 captured from hydrogen production (Shell, Pernis) and bioethanol production (Alco, Europoort). Surplus winter CO_2 (approx. 500kt/year) can be stored without installing additional capture equipment. There are other hydrogen facilities and waste incineration plants in the vicinity that could potentially also be connected to the CO_2 network (Maasvlakte CCS Project, 2017).

For the Port of Rotterdam, having an additional storage location, like Q16-Maas has great benefit. So, should this project be sanctioned, they would be willing to take up the expenses for the onshore transport.

7.1.2. Surface Facilities and Subsidies

Oranje-Nassau Energie and partners have estimated additional surface facilities to cost between €10M and €20M. This is primarily for a compressor that can inject CO_2 in the desired quantities and pressure. The operating expenses (OPEX) is estimated to be €18M over 2 years of injection.

As this is considered a European pilot, some subsidies have been approved for this project to stimulate its development. The European Economic Programme for Recovery (EEPR) has appointed €180M to this project and the Dutch government is willing to subsidise a maximum of €150M. The two power plant partners are also willing to subsidise the project with €100M. These subsidies, totalling €330M, are also expected to be used to fund the CO_2 capture process of this project, which is expected to be the most expensive part.

7.1.3. Well and Well Intervention Costs

Oranje-Nassau Energie has conducted a study to determine the additional costs for a completion to be made CO_2 injection ready. The additional costs are made up of the changes made to the Surface wellhead and tree, the installation of a 4.1/2" 25Cr tubing, the change of subsurface safety valve, packer, nipples and downhole gauges to 25 Cr quality. Also rig up, well kill, completion pull, clean out and rig down are included in the costs. Total cost for the workover are estimated to be €3.5M.

Well engineers of Oranje-Nassau Energie have estimated the costs of side-tracking the original well to be 8.5 million euros. Included in this estimate are materials and drilling costs, as well as a standard production completion. In case the completion needs to be ready of CO_2 service an additional €2.5M is required.

7.1.4. Monitoring of the Well

As the idea of this injection study is that it can be used as a pilot, monitoring the field over time is important to compare simulation results with real downhole values. Top seal integrity is assumed intact as long as no abnormal behaviour of pressure is observed. Pressure and temperature should be monitored to show no significant changes in expected values are measured. This can either be done with a permanent sensor or with memory gauges. As a wireline trip will be necessary for memory gauges, this can be combined with a reservoir saturation tool (RST), which measure carbon and oxygen concentrations, to track the CO_2 concentrations around the well in the reservoir. This should be tracked roughly every 6 to 12 months for a period of 5 years, after which a lower monitoring frequency would suffice for 15 additional years.

Also, the flow rate, pressure, temperature and composition of injected CO_2 impact the cold front inside the reservoir and impact stability of the faults. Injection pressure and temperature also determine the state of stress in the reservoir. Care should be taken not to exceed fracturing limits.

Microseismic activity in the caprock and at the faults should also be indicative for the integrity of the reservoir. Permanent geophones in the monitoring well should be placed to check this activity. CO_2 plume imaging can also be measured with seismic, but this would be too expensive to repeat each time, hence permanent geophones may be a good option together with an RST tool. (TNO, 2017) The monitoring costs will not be considered for this case study but should be accounted for once the CO_2 is securely stored.

7.2. Results

7.2.1. Sidetrack Potential

The Q16-Maas sales gas has a gross heating value of 42.63MJ/Nm^3 (≈ 40.41MJ/sm^3), which is 121% the Groningen value. The gas price is assumed to be the 121% the price of Groningen gas, that is 0.21euro/m^3 (including inflation) during the time of production. The condensate has a density of 0.7342 tonne/m^3 and an average price of 386euro/tonne. The condensate density and price takes the LPG sales into account and is the combined density and price of the two. Both price assumptions are taken from oil price forecast (confidential) models by Oranje-Nassau Energie for the year 2018. No depreciation over time will be considered as all investments happen within a year and the extra production only lasts a maximum of 2 years.

Table 12 below shows the oil production that also came with the different sidetrack scenarios. The income is simply the gas and oil production multiplied with the accompanying price. An OPEX of €9M/y is assumed. The costs are made up of the OPEX and CAPEX of the sidetrack and surface investments. The profit is the difference between the income and the costs.

Pore	Rel Perm	Gas production [sm^3]	Oil Production [sm^3]	= Oil [tonnes]	Sales Income [M€]	Costs [M€]	Profit [M€]
0,93	SOF3_NEW	1,66E+08	2,40E+04	1,76E+04	41,57	18,25	23,32
0,93	SOF3	1,83E+08	2,60E+04	1,91E+04	45,79	19,75	26,04
0,93	RAD	1,62E+08	2,28E+04	1,67E+04	40,56	17,50	23,06
0,96	SOF3_NEW	1,92E+08	2,80E+04	2,05E+04	48,26	20,50	27,76
0,96	SOF3	2,14E+08	3,03E+04	2,23E+04	53,49	22,00	31,49
0,96	RAD	1,88E+08	2,62E+04	1,93E+04	46,83	17,50	29,33
1	SOF3_NEW	2,21E+08	3,21E+04	2,36E+04	55,57	22,00	33,57
1	SOF3	2,45E+08	3,51E+04	2,57E+04	61,44	23,50	37,94
1	RAD	2,15E+08	2,99E+04	2,19E+04	53,65	18,25	35,40

Table 12. Sidetrack production sales and profit forecasts

As can be seen, each scenario is highly profitable, on average roughly €30M (before tax). The preferred (and least profitable) case, 0.93 pore factor and fit for purpose relative permeability curves, still shows a profit of €23M. The probability of success, a measure of technical and geological success for finding hydrocarbons, is very high for this case as the reservoir has already been tapped. It is highly recommended to continue with this course of action.

7.2.2. CO_2 Transport and Storage Break-even Point

The reason that a lot of subsidies are promised is that this is a pilot to prove the concept of CO_2 storage in depleted reservoirs. So, if CO_2 storage in depleted reservoirs were to really kick-off and become common practise, the subsidies may not be relied on for further CO_2 storage investments. The cost calculations are done with and without subsidies to show respectively, the break-even CO_2 storage price per tonne for the current pilot and if it were considered to be an investment for the future, with no subsidies. For the results shown below, some assumptions are made:

- The sidetrack option is chosen. The simultaneous injection and production strategy did not show potential. The original well could not store as much CO_2 and as the sidetrack option is already considered the actual course of action, this option is more relevant to explore.
- The cost of the completion for the sidetrack for CO_2 injection, after normal production, was assumed to be €3.5M. The OPEX of injecting CO_2 is considered to be the same as during production of the field, namely €9M/year.
- The high-case CAPEX is €53.5M and the low-case CAPEX is €43.5M. Over a two year injection span, this gives a total cost of €71.5M for the high-case and €61.5M for the low-case costs.

Table 13 shows the results of calculating the break-even point for which CO_2 storage and transport costs cover the expenses.

Pore	Rel Perm	BHP limit	CO_2 Injected[kg]	High-case break-even (€/tCO_2)	Low case break-even (€/tCO_2)	OPEX break-even (€/tCO_2)
0,93	SOF3_NEW	290	1,36E+09	52,59	45,24	13,24
0,93	SOF3	290	1,35E+09	52,80	45,42	13,29
0,93	RAD	290	1,38E+09	51,99	44,72	13,09
0,96	SOF3_NEW	290	1,40E+09	51,24	44,07	12,90
0,96	SOF3	290	1,39E+09	51,38	44,19	12,93
0,96	RAD	290	1,41E+09	50,73	43,63	12,77
1	SOF3_NEW	290	1,44E+09	49,58	42,64	12,48
1	SOF3	290	1,42E+09	50,20	43,18	12,64
1	RAD	290	1,45E+09	49,26	42,37	12,40
0,93	SOF3_NEW	290 + 2 years	1,70E+09	52,50	46,64	21,12
0,93	SOF3_NEW	310	1,75E+09	40,95	35,22	10,31
0,93	SOF3_NEW	310 + 2 years	2,35E+09	38,06	33,81	15,31
0,93	SOF3_NEW	330	1,87E+09	38,29	32,94	9,64
0,93	SOF3_NEW	330 + 2 years	2,97E+09	30,13	26,77	12,12

Table 13. Sidetrack injection costs/storage volume

The high-case and low-case break-even prices per volume, show the price of storing the CO_2 in this reservoir if no subsidies are granted and only transport and storage costs are considered. If only the CAPEX were subsidized the resulting break-even price/volume is shown in the last column. When inspecting the results of Table 13, a few things can be noted:

- Injecting more CO_2 in the same amount of time, logically, reduces the break-even point. This is why injecting with a higher BHP limit is more cost effective.
- Injecting for 2 additional years reduces the break-even price for the total costs, but if you look solely at the OPEX, the injection does not outweigh the operational costs. The operational costs are too high to compensate for the additional injected CO_2. Only if storing at higher prices then calculated is possible, is this a viable option.

- The fact that the subsidies cover or should nearly cover the expenditure is instrumental for the feasibility of storage in the Q16-Maas field.

The added benefit of delayed costs of abandonment for the joint venture operating this field, if they would remain operator when injecting CO_2, was not considered.

8. Conclusions and Discussion

8.1. Conclusions

The trapping of CO_2 and containing it in a depleted reservoir needs to be secure and safe storage needs to be guaranteed. A literature review has been conducted to study the storage capabilities of Q16-Maas and research the effects of injecting CO_2 into a gas condensate reservoir. The following conclusions can be drawn from the literature review:

- Gas reservoirs have a proven track record for safely trapping gaseous phases in the subsurface over long geological timescales. As long as initial reservoir conditions are not exceeded too much, CO_2 in supercritical phase should be safely stored.
- With increasing time, the CO_2 is trapped more securely.
- The strategic location of the Q16-Maas field makes it very interesting for CO_2 storage. Its onshore facility, close to the industrial port of Rotterdam, makes it easy to connect to the already existing CO_2-network and would make the transport component of this CCS project low-cost. The offshore field location also limits the geopolitical issues that came with cancelled onshore CO_2 storage fields like Barendrecht.
- CO_2 injection for enhanced hydrocarbon recovery has been practised on a commercial scale for nearly 50 years. Repressurizing of the reservoir can vaporize condensed hydrocarbons and alleviate condensate blockage. It also minimises surface tension that exists between gas and liquid phase and frees the trapped condensate. CO_2 flooding is also successfully deployed in oil reservoir. Injected CO_2 pushes unswept oil through the reservoir to the producers.

The idea for CO_2 storage in Q16-Maas first came when the large aquifer influx into the reservoir was not considered. Initial studies determined that over 2 million tonnes of CO_2 could be stored in this reservoir. The presence of the strong aquifer, calculated to be 600Mm^3 in volume, tremendously reduces the amount of storage capacity. The water influx prematurely drowned production from the original well. Sidetracking of the original well, updip in the formation from the current location, would tap the attic gas that remains. By simulating the dynamic reservoir conditions in Eclipse E300, a study has been done to explore this possibility.

- Additional gas production ranging between 162 million sm^3 and 245 million sm^3 can be extracted by means of sidetracking the well and tapping into remaining attic gas.
- The resulting additional profit of producing untapped gas and condensate by means of a sidetrack is roughly €23M-€37M (before tax).
- The possibility of success of such an opportunity is very high as the presence of gas has already been proven.

If the sidetrack is considered to be a completely new well, enhanced hydrocarbon recovery may be possible. Two scenarios were tested. First, the sweep of the water may be improved by injecting CO_2 ahead of the front. Second, immobilized condensate that dropped out in the Röt may be respressurized, consequently becoming more mobile and leading to increased condensate production.

- The injecting of CO_2 ahead of the water did not show any significant increase in production. The sweep of the water can be considered to be very effective and injecting CO_2 for the purpose of enhancing recovery is unprofitable and does not show better potential than the water sweep naturally occurring.

- For repressurizing and mobilizing valuable condensate in the Röt formation, the thickness of the layer impedes any such enhanced condensate recovery. The injected CO_2 quickly breaks through in the production well, that consequently will lead to unwanted and expensive separation processes.

When considering CO_2 storage, both the original well production and the sidetrack production strategies were considered. Both scenarios considered CO_2 could only be injected from 2020 onwards, and would be injected for 2 years.

- If the MSG-03X well is considered to be the injection well, only 50% of the initially calculated CO_2 can be stored (roughly 1.05Mt).
- By sidetracking the MSG-03X well and producing additional hydrocarbons, not only can more CO_2 be stored (roughly 1.4Mt) but also a sound investment can be done. The attic gas remaining is significant enough to produce from and pay back the investment of the sidetrack.
- The repressurizing of the reservoir due to water influx from the aquifer negatively influences the amount of storable CO_2. The bottomhole limit restriction, set to ensure safe trapping, is reached quicker if the reservoir is at a higher initial injection pressure.

Concluding, a study is done on the costs of transporting CO_2 and storing it in the Q16-Maas field to show the investment costs that need to be made for such a project. This does not consider the most expensive investment, the capturing of CO_2. As the sidetrack is considered to be implemented due to the positive investment potential it has, this is considered for the cost analysis.

- The high-case CAPEX is €53.5M and the low-case CAPEX is €43.5M. The OPEX of injecting CO_2 is considered to be the same as during production of the field, namely €9M/year. Over a two-year injection span, this gives a total cost of €71.5M for the high-case and €61.5M for the low-case costs.
- Assuming a storage volume of 1.4 million tonnes, the costs that need to be covered per injected tonne of CO_2 varies between 52.5€/tCO_2 and 42.5€/tCO_2.
- By increasing the bottomhole pressure limit restriction, more CO_2 can be stored and this also reduces the cost per storable volume. If the injection time in combination with a higher pressure limit is also increased, the costs can be reduced to roughly 26.7€/tCO_2, but comes with more risk as the initial reservoir pressure is exceeded.

With the European Union's Emissions Trading System, a policy was started to combat climate change and reduce gas emissions cost-effectively. The price of emitting CO_2 however has not significantly risen to levels that were expected. If the industry is willing to pursue the storage of CO_2 into depleted reservoirs, the carbon capture, transport and storage costs need to be lower than the cost of emitting CO_2. This case study has shown the importance of having higher EU CO_2 emitting costs to get industries to consider storing CO_2 as a cheaper option than emitting it. The investments need to be covered by means of subsidies because the costs are simply too high at the moment.

8.2. Discussion

Since the start of the case study, a lot of developments have happened surrounding this project. Firstly, in June of 2017, Uniper and ENGIE, the powerplants and promoters of this project have backed out of the project. The costs of capturing the CO_2 is too high and, with the low-emission costs, not profitable to pursue. As the location of the power plants was so close to the Q16-Maas facility it was a good option to go with. Luckily, Rotterdam's industrial harbour has enough other options, from which CO_2 could be captured and is still considered nearby, but will slightly increase transportation costs.

The new 'regeerakkoord', the coalition plan for the new Dutch cabinet, presented in October of 2017, has very ambitious CO_2 capture and storage plans. In 2030, the coalition wishes to capture 20 million tonnes of CO_2 annually. Considering the results from this research, the costs of such projects are too high and reaching the goals would cost a tremendous amount of money. With experience and a CO_2 network costs may be reduced, but will still cost a lot of money.

As mentioned in section 7.1.1, a CO_2 network already exists for the greenhouses surrounding Rotterdam. 'Organic CO_2 for assimilation by plants' (OCAP) is a joint venture between gas supplier Linde Gas and construction group VolkerWessels that delivers roughly 300000 tonnes of pure CO_2 to the greenhouses in Westland, Lansingerland, Delfgauw and Wilgenlei. The CO_2 that is produced in Rotterdam harbour, is collected and transported to those areas. During the summer peak months, the demand for CO_2 is higher than the available supply, whilst during wintertime too much CO_2 is available. OCAP has recognised the potential of using the Q16-Maas field as a buffer for this need of surplus of CO_2.

8.3. Recommendations and Further Research

With the Dutch government relying heavily on CO_2 storage for reaching their climate goals, pilots like the ROAD project should be conducted. By gaining actual field experience and expertise in CO_2-injection pilots, future projects can be assessed and presented with more certainty. The findings of this study are all theoretical and comparing the theoretic outcome to the simulations can give a better understanding of how to best model future CO_2 storage projects.

For further research, the same models could be run without the aquifer presence, as this strongly reduces the storable CO_2 because of its repressurizing of the reservoir. The strong aquifer influx seen in this reservoir is not as significant in other reservoirs, so simulating without this aquifer volume could give interesting insights into other field potentials and modelling strategies. Expanding on this topic, one could even go so far as to investigate the optimal timing of injection to maximize storage capacity for any gas reservoir that has aquifer support.

With the research done by Oranje-Nassau Energie on the additional well costs, in section 7.1.3, the additional costs of also including a CO_2-injection resistant liner were not considered. The perforated liner could corrode because of the injected CO_2 and the effects needs to be researched. Other near wellbore effects were also not considered, like the Joule-Thomson effect. The 'benefit' of having a reservoir that is repressurized by the aquifer influx means that these effects have less impact on the injection as the pressure difference is less. Furthermore, this case study was a study on macroscopic scale and near wellbore effects are considered microscopic. But as this could still be problematic, research may be necessary.

9. References

Bloomberg View. (2017). *Europe Needs a Higher Price on Carbon.* Retrieved from https://www.bloomberg.com/view/articles/2017-02-20/europe-needs-a-higher-price-on-carbon.

Blunt, M. (2010). Carbon Dioxide Storage. *Grantham Institute for Climate Change Briefing paper No 4*.

CoreLab Reservoir Optimization. (2011). *Reservoir Fluid Analyisis for Oranje-Nassau Energie MSG-03X, Final Report.*

Dake, L. (Volume 8, 1st edition). Fundamentals of Reservoir Engineering. Elsevier.

Essandoh-Yeddu, J., & Gülen, G. (2009). *Economic modeling of carbon dioxide integrated piepeline network for enhanced oil recovery and geologic sequestration in the Texas Gulf Coast region.* Energy Procedia 1.

Fan, L., Harris, B. W., Jamaluddin, A., Kamath, J., Mott, R., Pope, G. A., . . . Whitson, C. (2005). Understanding Gas-Condesate Reservoirs. *Oil Field Review*, 14-27.

Global CCS Institute. (2009). Retrieved from https://hub.globalccsinstitute.com/publications/strategic-analysis-global-status-carbon-capture-storage-report-1/d1-co2-storage

Global CCS Institute. (2016a). *The Global Status of CCS, Summary Report.* Global CCS institute.

Global CCS Institute. (2016b, September 20). Retrieved from https://www.globalccsinstitute.com/projects/sleipner%C2%A0co2-storage-project

Holloway, S. (1996). An Overview of the Joule II Project 'The Underground Disposal of Carbon Dioxide'. *Energy Conversion Management (37)*, 1149-1154.

IEA. (2015). *Storing CO2 through Enhanced Oil Recovery.* International Energy Agency.

Kurdi, M., Xiao, J., & Liu, J. (2012). Impact of CO2 Injection on Condensate Banking in Gas Condensate Reservoirs. Society of Petroleum Engineers.

Maasvlakte CCS Project. (2017). *An Immdiate Start to Industrial CCS in Rotterdam.*

Narinesingh, J., & Alexander, D. (2014). CO2 Enhanced Gas Recovery and Geologic Sequestration in Condensate Reservoir: A Simulation Study of the Effects of Injection Pressure on Condensate Recovery from Reservoir and CO2 Storage Efficiency. *Energy Procedia (63)*, 3107-3115.

Oranje-Nassau Energie. (2017). *Well proposal MSG-03Y.*

Price, J., & Smith, B. (2008). *Geological Storage of Carbon Dioxide, Staying Safely Underground.* International Energy Agency (IEA).

PTRC. (2014). *What Happens When CO2 is Stored Underground - Q&A from the IEAGHG Weyburn-Midale CO2 Monitoring and Storage Project.* Melbourne: Global Carbon Capture and Storage Institute Limited.

Road2020.nl. (2017). *Road CCS*. Retrieved from http://road2020.nl/en/

Schlumberger. (1994). *Saturation Monitoring With the RST Reservoir Saturation Tool.*

Schlumberger. (2014). *Eclipse Technical Description.*

Seo, J. G. (2004). *Experimental and Simulation Studies of Questration of Supercritical Carbon Dioxide in Depleted Gas Reservoirs.* Texas A&M.

Shtepani, E. (2006). CO2 Sequestration in Depleted Gas/Condensate Reservoirs. *SPE Annual Technical Conference and Exhibition*, 24-27.

Span, R., & Wagner, W. (1996). A New Equation of State for Carbon Dioxide Covering the Fluid Region from the Triple-Point Temperature to 1100 K at Pressures up to 800 MPa. *Journal of Physical and Chemical Reference Data 25 (6)*, 1509-1596.

Tan, J. (2012). *Co-optimising CO2 Storage and Enhanced Recovery in Gas and Gas Condensate Reservoirs.* Sydney: UNSW Australia, School of Petroleum Engineering.

TNO. (2017). *Q16-Maas Monitoring Final report (confidential).*

Vandeweijer, V., van de Meer, B., Hofstee, C., Mulders, F., D'Hoore, D., & Hilbrand, G. (2011). K12-B, CO2 storage and enhanced gas recovery. *Energy Procedia 4*, 5471-5478.

Veenhof, R., & Mullink, J. (2012). *Field Development Plan Q16-Maas.* ONE.

Xodus Advisory. (2016). *ONE Reservre Audit 2016 Q16-Maas.*

Zaluski, W., El-Kaseeh, G., Lee, S.-Y., Piercey, M., & Duguid, A. (2016). Monitoring technology ranking methodology for CO2-EOR sites using the Weyburn-Midale Field as a case study. *International Journal of Greenhouse Gas Control (54)*, 466-478.

10. Nomenclature

$\bar{c}$	total aquifer compressibility
c_f	pore compressibility
c_w	water compressibility
J	Productivity index
k_r	relative permeability
$\bar{p}_a$	average aquifer pressure
p_{BH}	bottomhole pressure
P_c	capillary pressure
p_D	dewpoint pressure
p_i	initial pressure
p_{nw}	pressure of non-wetting phase
p_w	pressure of wetting phase
r	radius
t	time
W_e	cumulative water influx
W_{ei}	initial amount of encroachable water in an aquifer
σ	interfacial tension

11. Appendices

11.1. Appendix A

Flowing (P) and Shut-in (S) Comparison PLT/MPLT Log (S1P1: 01-06-2016 & S3P3: 09-10-2016) MSG-03X

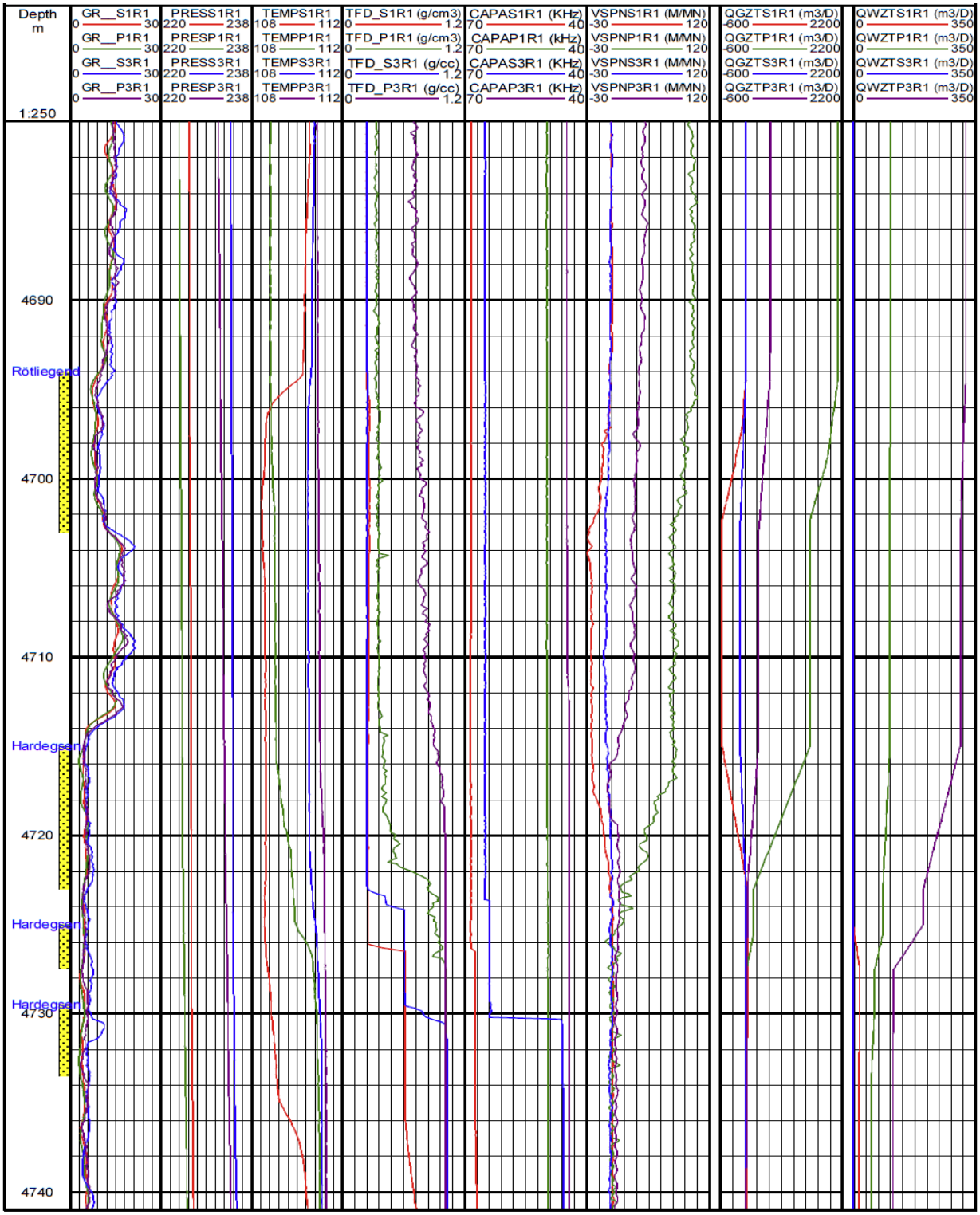

11.2. Appendix B

RST (Reservoir Saturation Tool) data

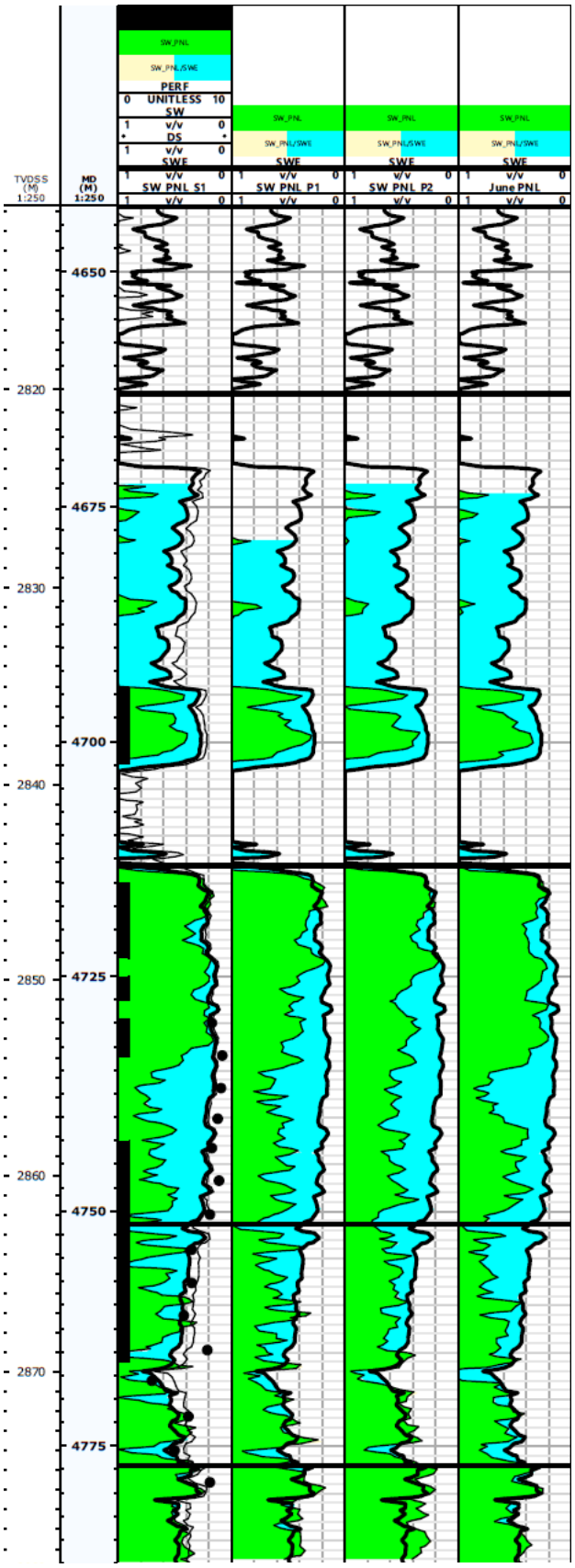

11.3. Appendix C

Gas relative permeability curves and water relative permeability curves

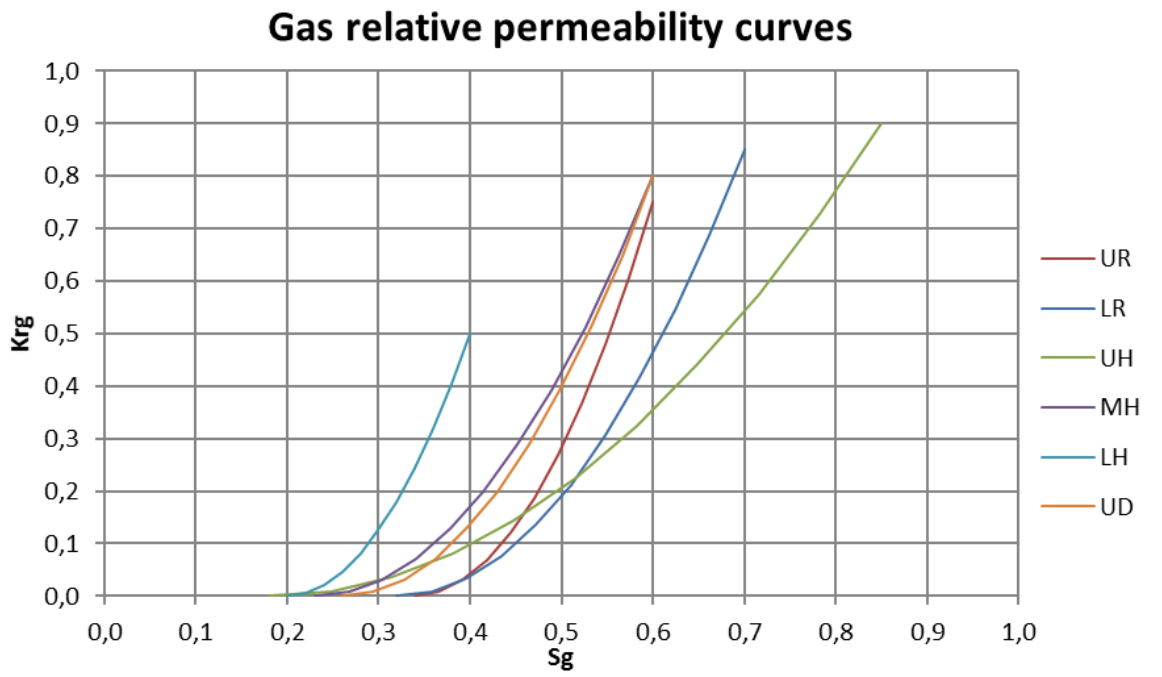

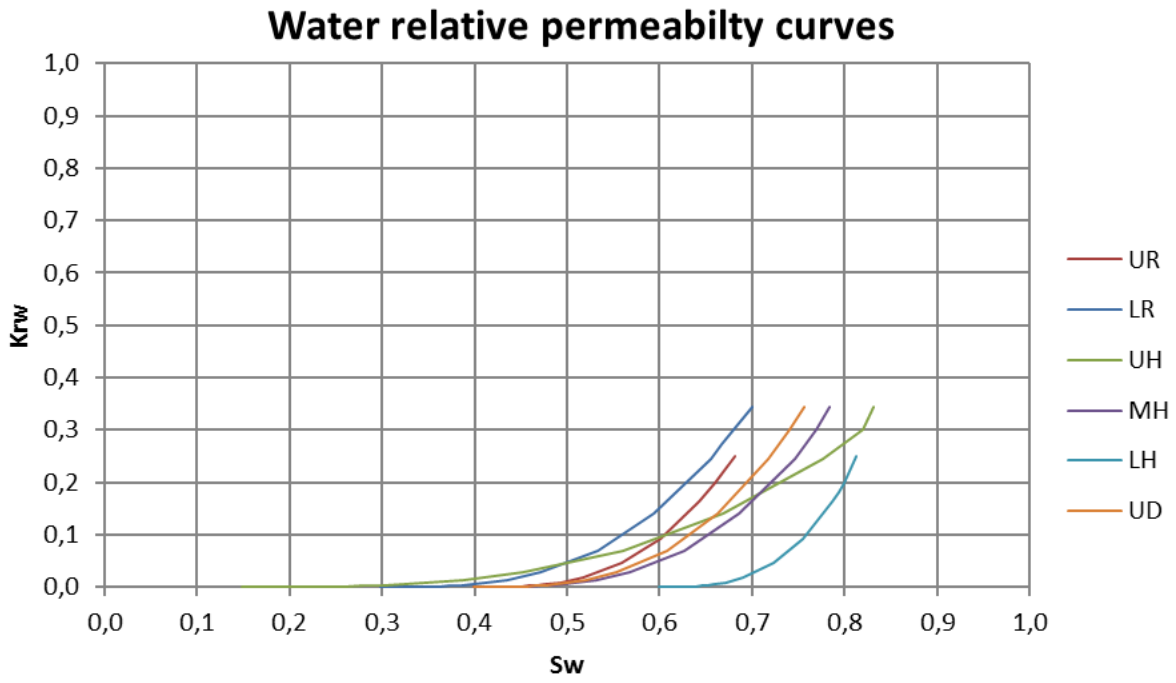

11.4. Appendix D

Calculated Uncontaminated Composition of Open Hole Sample (4723.9 m MD) to C36+

	Component	Mole %	Weight %
H_2	Hydrogen	0.00	0.00
H_2S	Hydrogen sulphide	0.00	0.00
CO_2	Carbon dioxide	0.54	0.90
N_2	Nitrogen	2.00	2.12
C_1	Methane	74.57	45.14
C_2	Ethane	9.18	10.41
C_3	Propane	4.90	8.15
iC_4	i-Butane	1.12	2.45
nC_4	n-Butane	1.52	3.33
C_5	neo-Pentane	0.01	0.03
iC_5	i-Pentane	0.63	1.72
nC_5	n-Pentane	0.57	1.55
C_6	Hexanes	0.75	2.43
	Me-Cyclo-pentane	0.14	0.44
	Benzene	0.05	0.16
	Cyclo-hexane	0.24	0.78
C_7	Heptanes	0.49	1.86
	Me-Cyclo-hexane	0.50	1.85
	Toluene	0.11	0.39
C_8	Octanes	0.52	2.22
	Ethyl-benzene	0.02	0.09
	Meta/Para-xylene	0.13	0.51
	Ortho-xylene	0.03	0.13
C_9	Nonanes	0.36	1.72
	Tri-Me-benzene	0.03	0.15
C_{10}	Decanes	0.33	1.78
C_{11}	Undecanes	0.26	1.42
C_{12}	Dodecanes	0.18	1.11
C_{13}	Tridecanes	0.17	1.12
C_{14}	Tetradecanes	0.12	0.89
C_{15}	Pentadecanes	0.11	0.85
C_{16}	Hexadecanes	0.08	0.66
C_{17}	Heptadecanes	0.07	0.62
C_{18}	Octadecanes	0.07	0.65
C_{19}	Nonadecanes	0.05	0.45
C_{20}	Eicosanes	0.03	0.36
C_{21}	Heneicosanes	0.03	0.30
C_{22}	Docosanes	0.02	0.25
C_{23}	Tricosanes	0.02	0.21
C_{24}	Tetracosanes	0.01	0.17
C_{25}	Pentacosanes	0.01	0.14
C_{26}	Hexacosanes	0.01	0.11
C_{27}	Heptacosanes	0.01	0.09
C_{28}	Octacosanes	0.01	0.08
C_{29}	Nonacosanes	0.00	0.06
C_{30}	Triacontanes	0.00	0.04
C_{31}	Hentriacontanes	0.00	0.03
C_{32}	Dotriacontanes	0.00	0.02
C_{33}	Tritriacontanes	0.00	0.02
C_{34}	Tetratriacontanes	0.00	0.01
C_{35}	Pentatriacontanes	0.00	0.01
C_{36+}	Hexatriacontanes plus	0.00	0.02
	Totals :	100.00	100.00

Note: 0.00 means < 0.005.

11.5. Appendix E

Constant Composition Expansion at 111.2°C

Pressure (bara)		Relative Volume (1)	Retrograde Liquid Volume % (2)	(3)	Density (g cm-3)	Deviation Factor Z	Calculated Gas Viscosity (cP) (4)
449.2		0.8113			0.3299	1.141	0.0424
414.7		0.8373			0.3197	1.087	0.0404
380.2		0.8704			0.3075	1.036	0.0381
345.8		0.9126			0.2933	0.988	0.0357
318.2		0.9545			0.2804	0.951	0.0336
311.3		0.9663			0.2770	0.942	0.0331
304.4		0.9787			0.2735	0.933	0.0326
297.5		0.9917			0.2699	0.924	0.0321
296.7	**Reservoir pressure**	**0.9932**			**0.2695**	**0.923**	**0.0320**
293.3	**Dew point pressure**	**1.0000**	**0.00**	**0.00**	**0.2677**	**0.918**	**0.0317**
290.6		1.0059	0.04	0.04			
287.1		1.0137	0.20	0.20			
283.7		1.0218	0.44	0.43			
269.9		1.0573	1.78	1.68			
256.1		1.0984	3.17	2.88			
242.3		1.1462	4.34	3.78			
207.9		1.3043	6.29	4.82			
173.4		1.5454	7.36	4.76			
138.9		1.9335	7.87	4.07			
107.8		2.5277	7.96	3.15			
83.8		3.3161	7.80	2.35			
57.3		4.9825					
38.7		7.5293					

(1) Relative Volume = V / Vsat ie. volume at indicated pressure per volume at dew point pressure.
(2) Retrograde liquid volume as a percentage of the volume at dew point pressure.
(3) Retrograde liquid volume as a percentage of the volume at indicated pressure.
(4) Calculated using the method of Lee, Gonzales and Eakin, JPT, Aug 1966.

11.6. Appendix F

Retrograde Liquid Curve During Constant Composition Expansion at 111.2°C

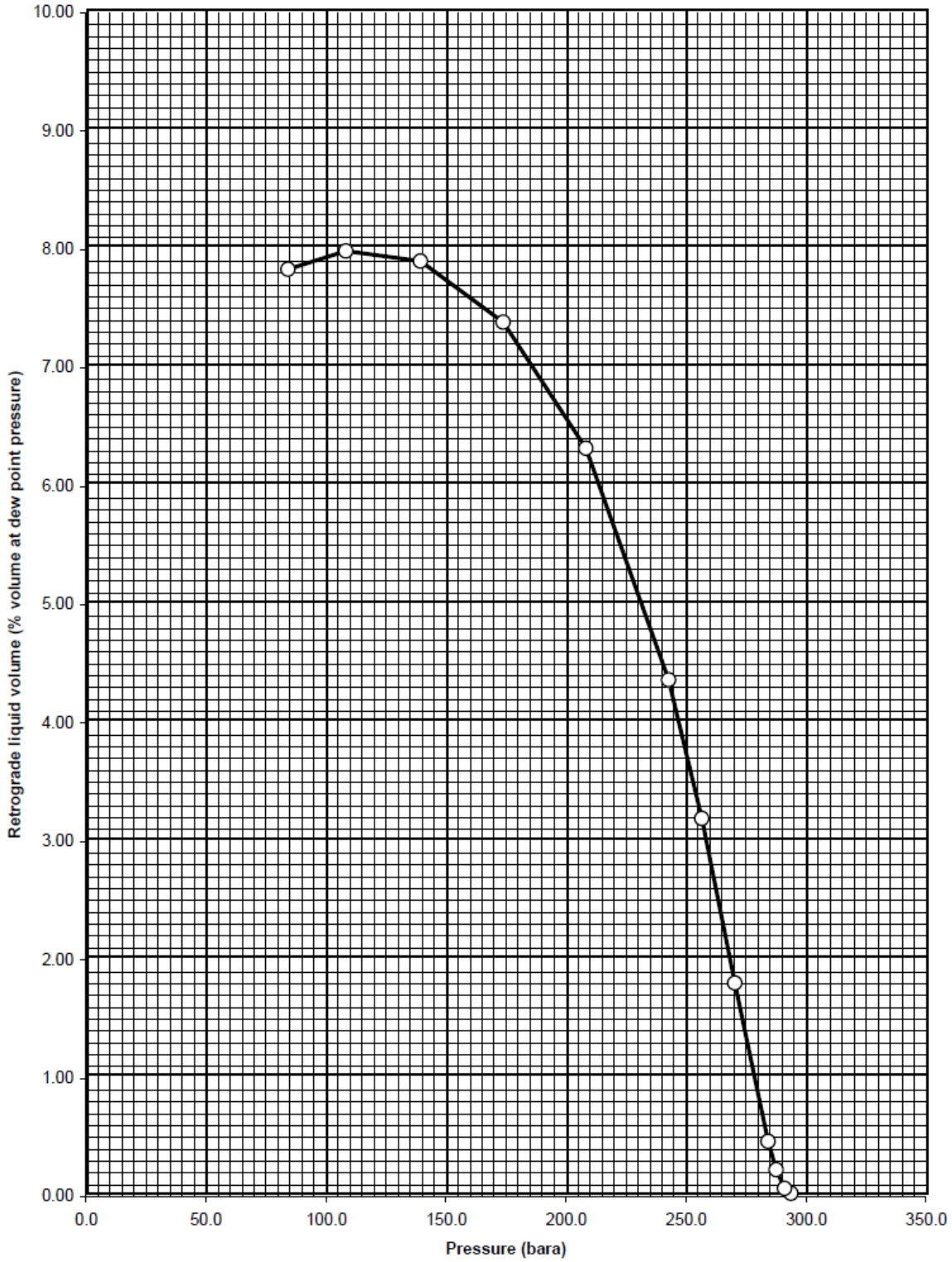

11.7. Appendix G – with sidetrack

Prod. & Inj. profile for 0.93 pore volume factor and radial model relative permeability curve

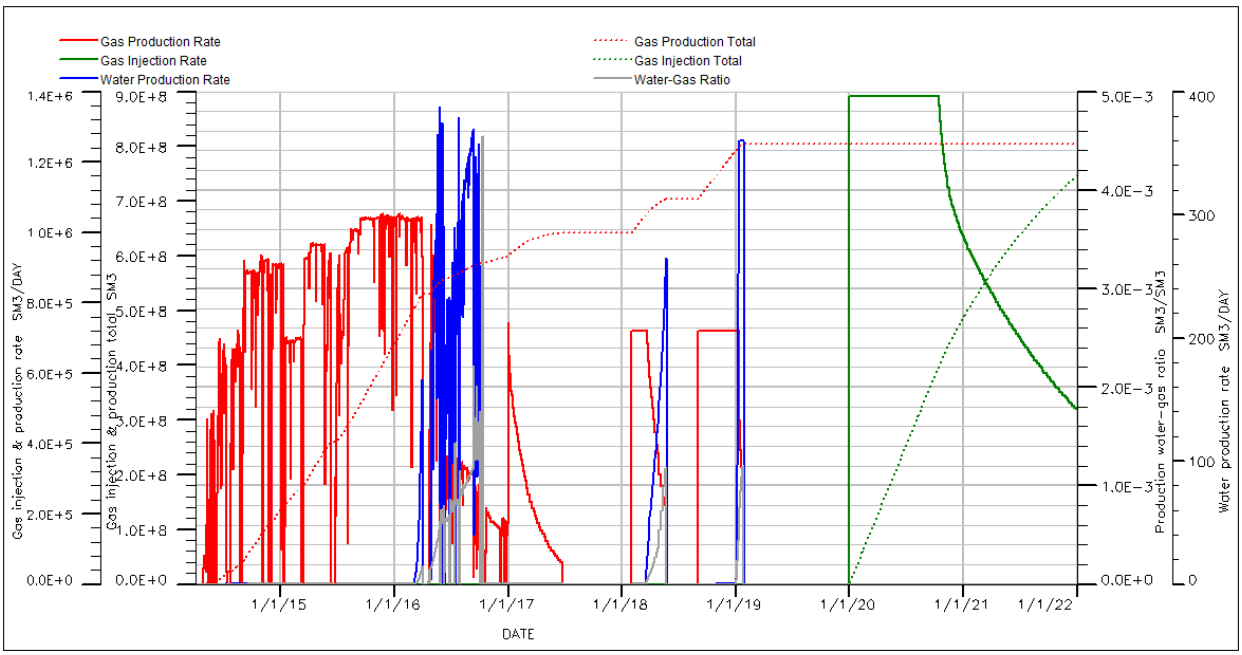

Prod. & Inj. profile for 0.93 pore volume factor and eclipse manual relative permeability curve

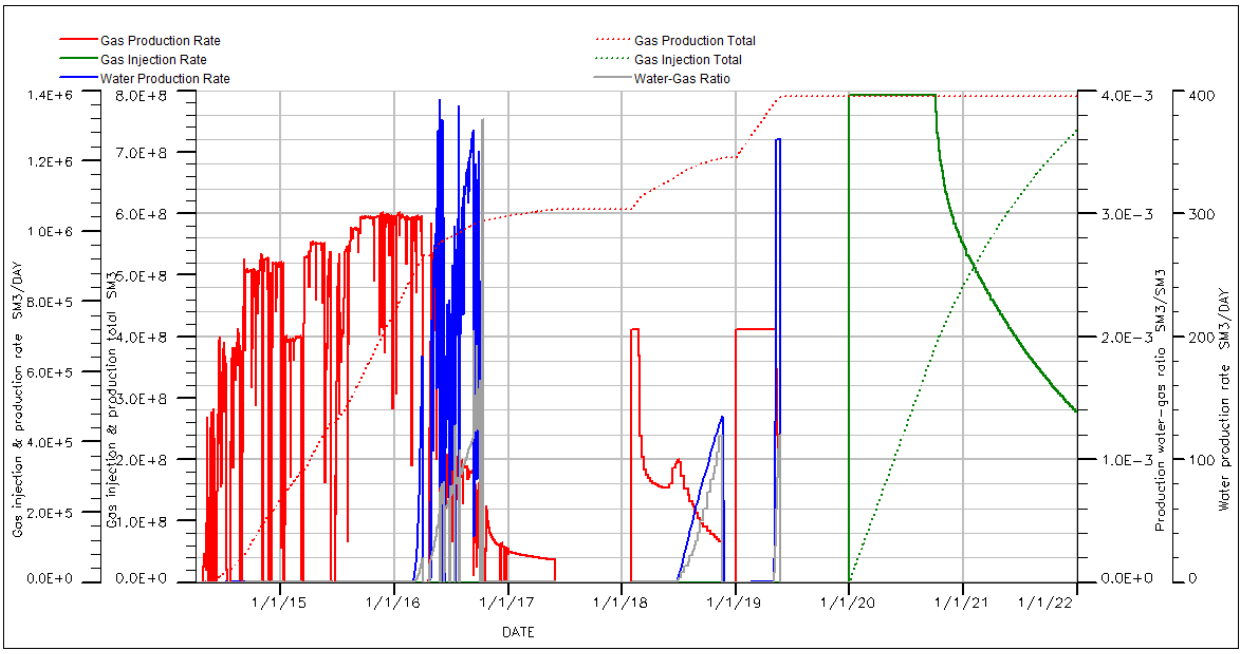

Prod. & Inj. profile for 0.93 pore volume factor and fit for purpose relative permeability curve

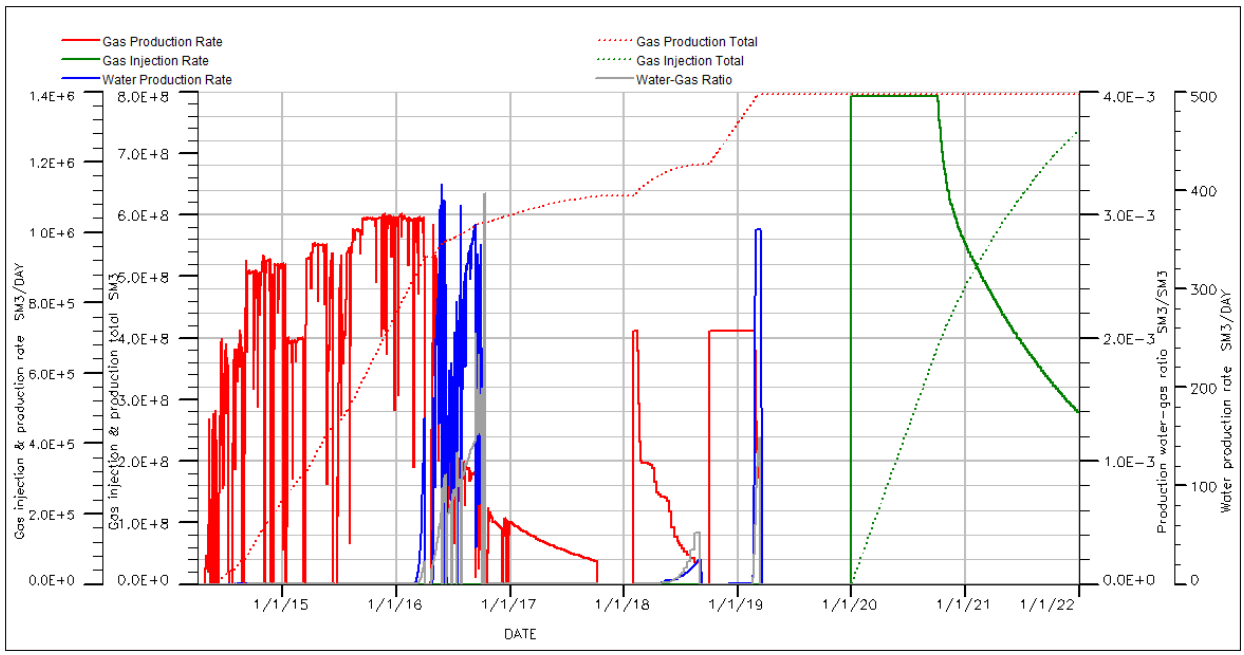

Prod. & Inj. profile for 0.96 pore volume factor and radial model relative permeability curve

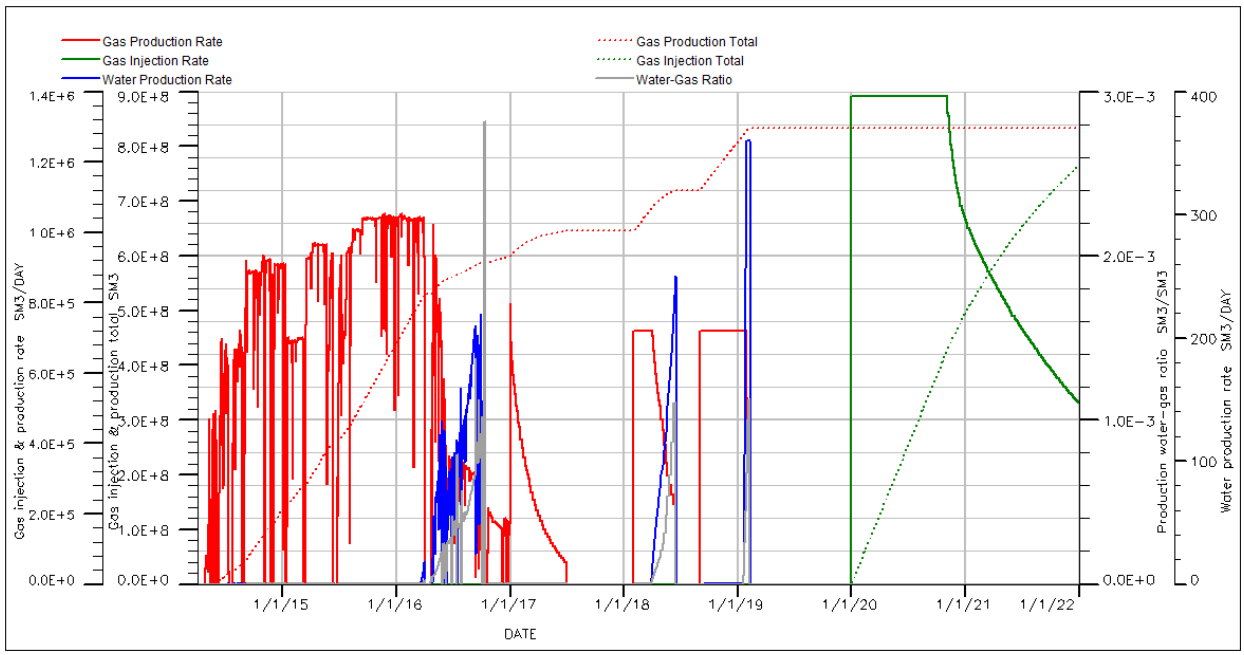

Prod. & Inj. profile for 0.96 pore volume factor and eclipse manual relative permeability curve

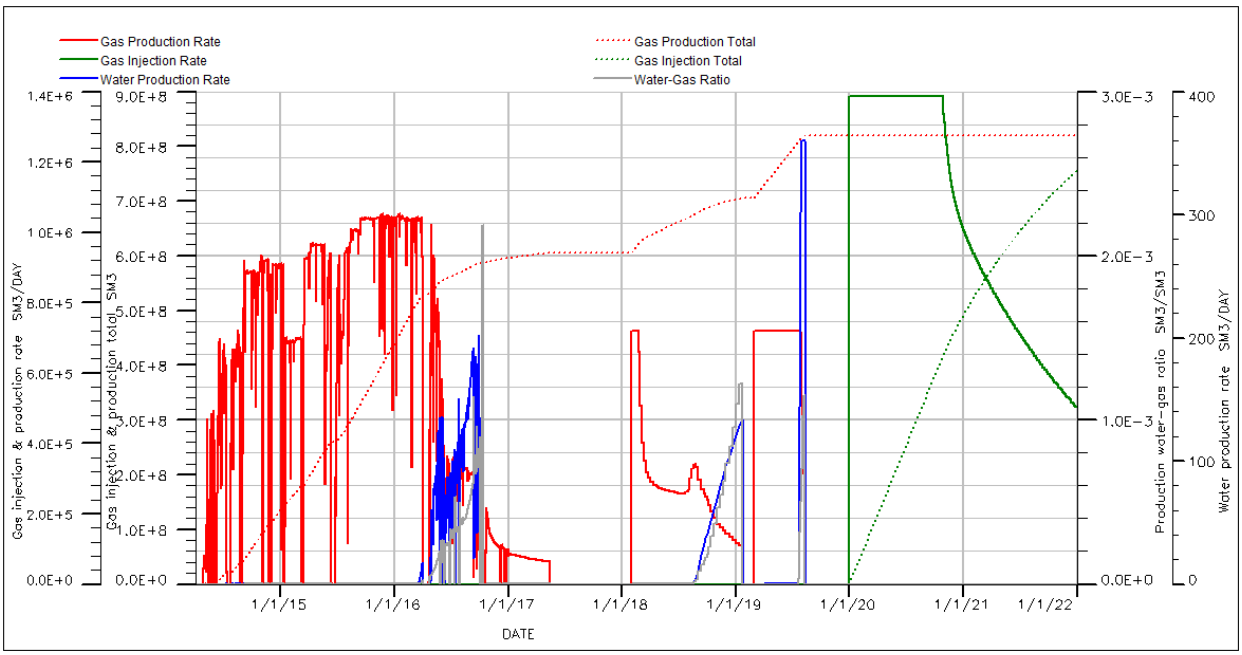

Prod. & Inj. profile for 0.96 pore volume factor and fit for purpose relative permeability curve

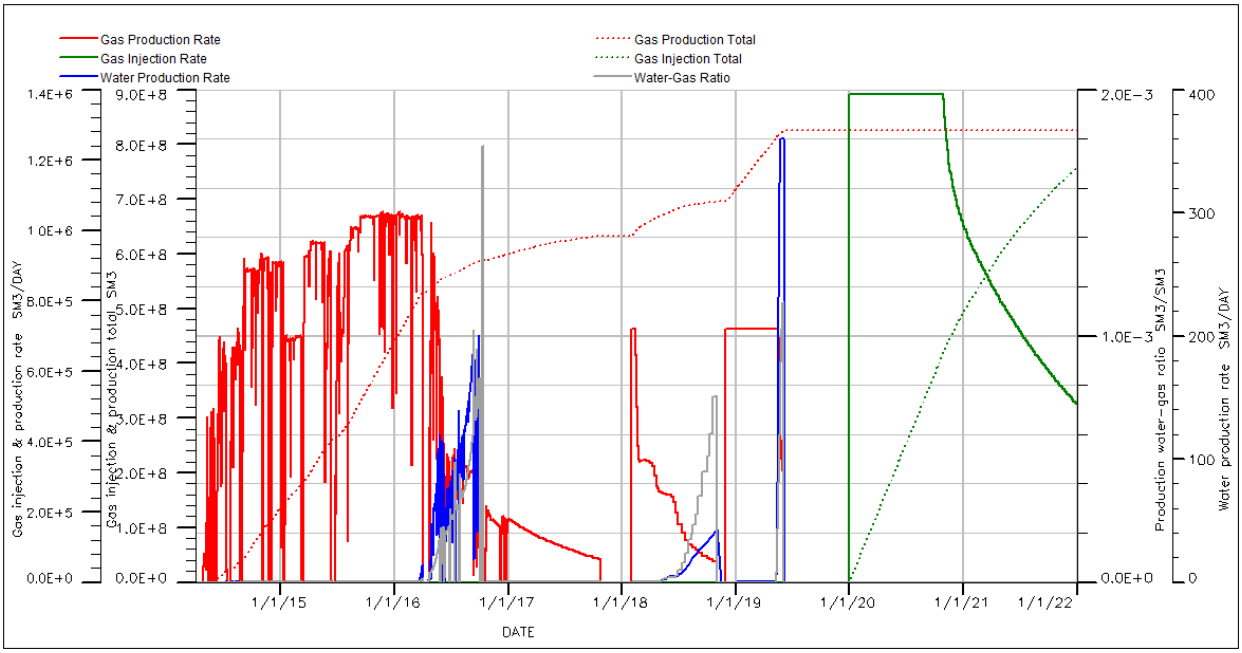

Prod. & Inj. profile for original pore volume factor and radial model relative permeability curve

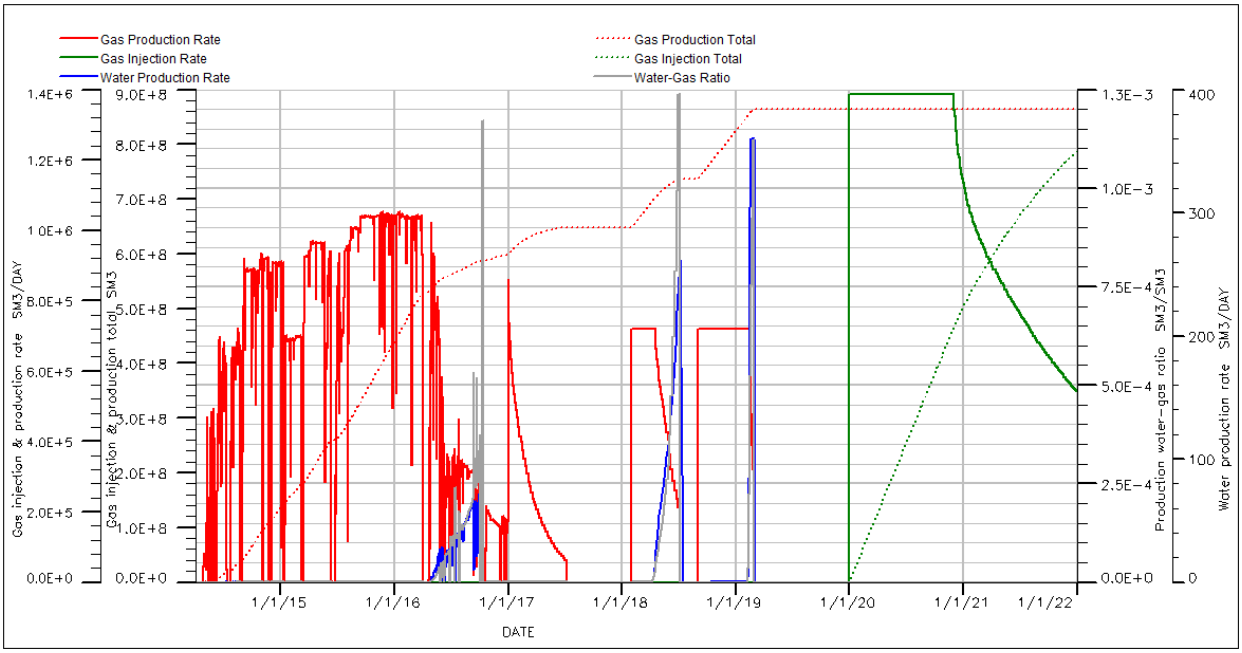

Prod. & Inj. profile for original pore volume factor and eclipse manual relative permeability curve

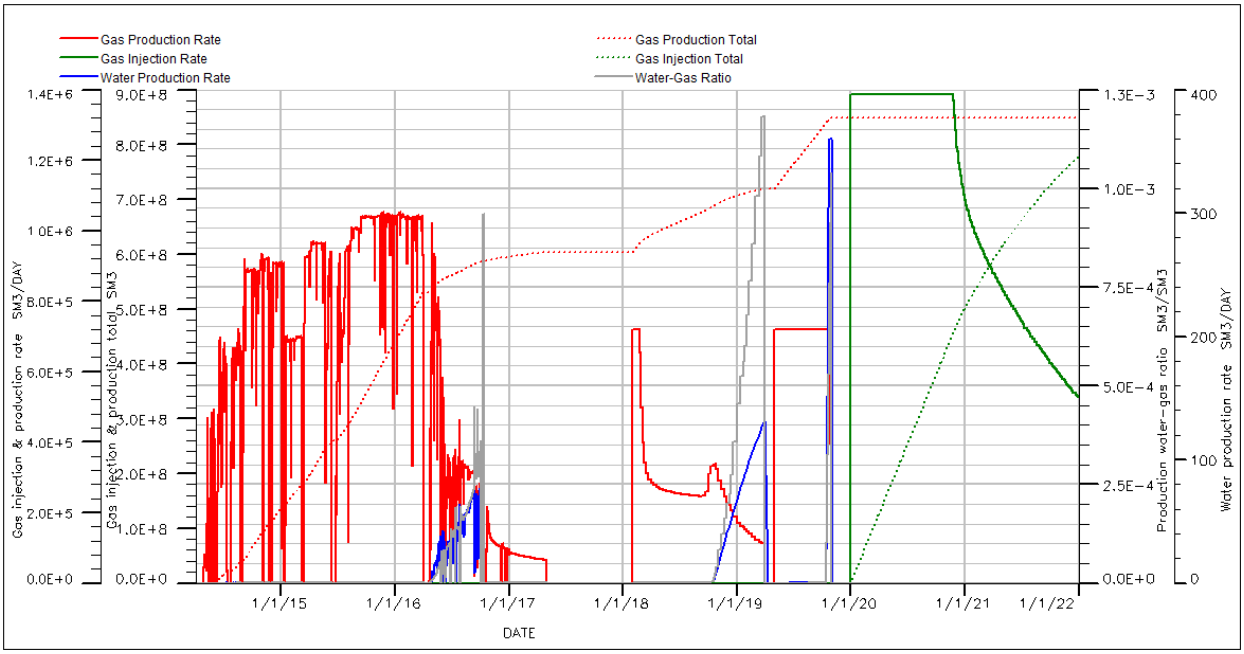

Prod. & Inj. profile for original pore volume factor and fit for purpose relative permeability

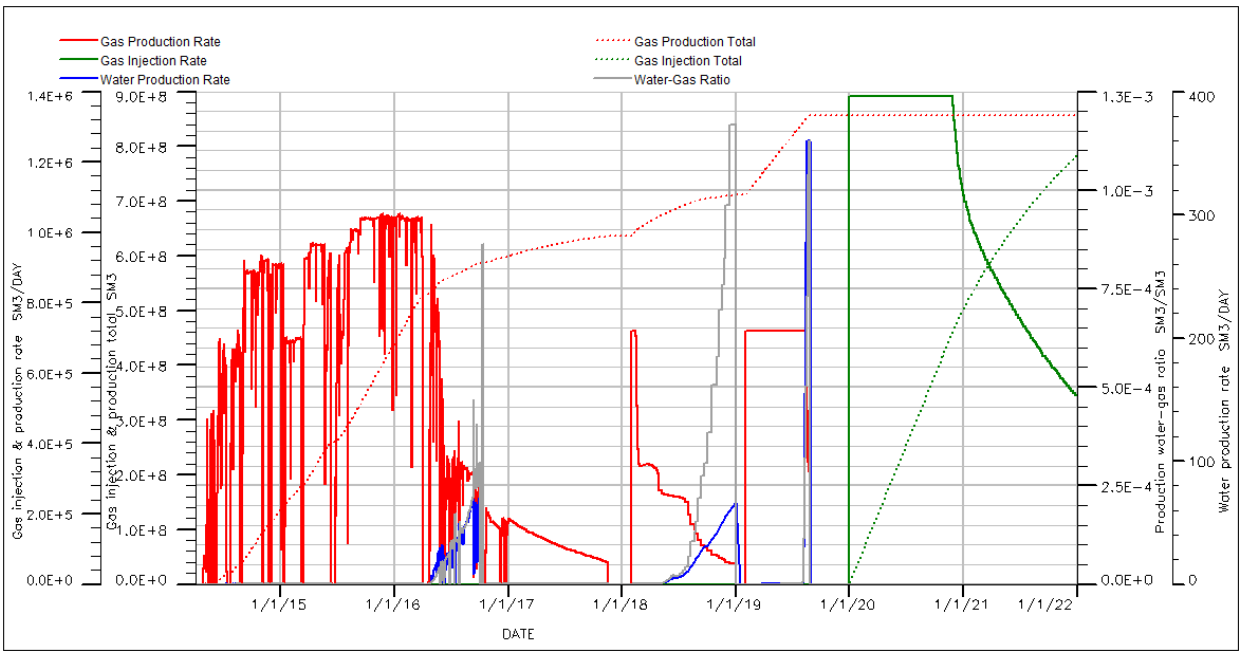

11.8. Appendix H – without sidetrack

Prod. & Inj. profile for 0.93 pore volume factor and radial model relative permeability curve

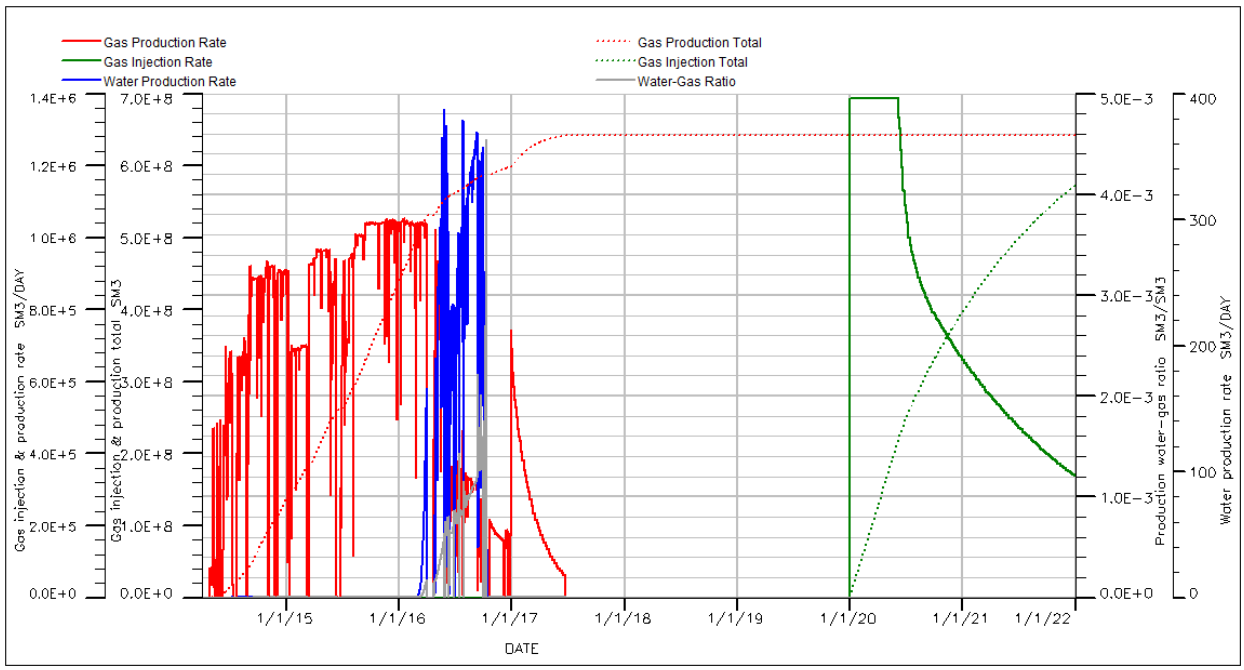

Prod. & Inj. profile for 0.93 pore volume factor and eclipse manual relative permeability curve

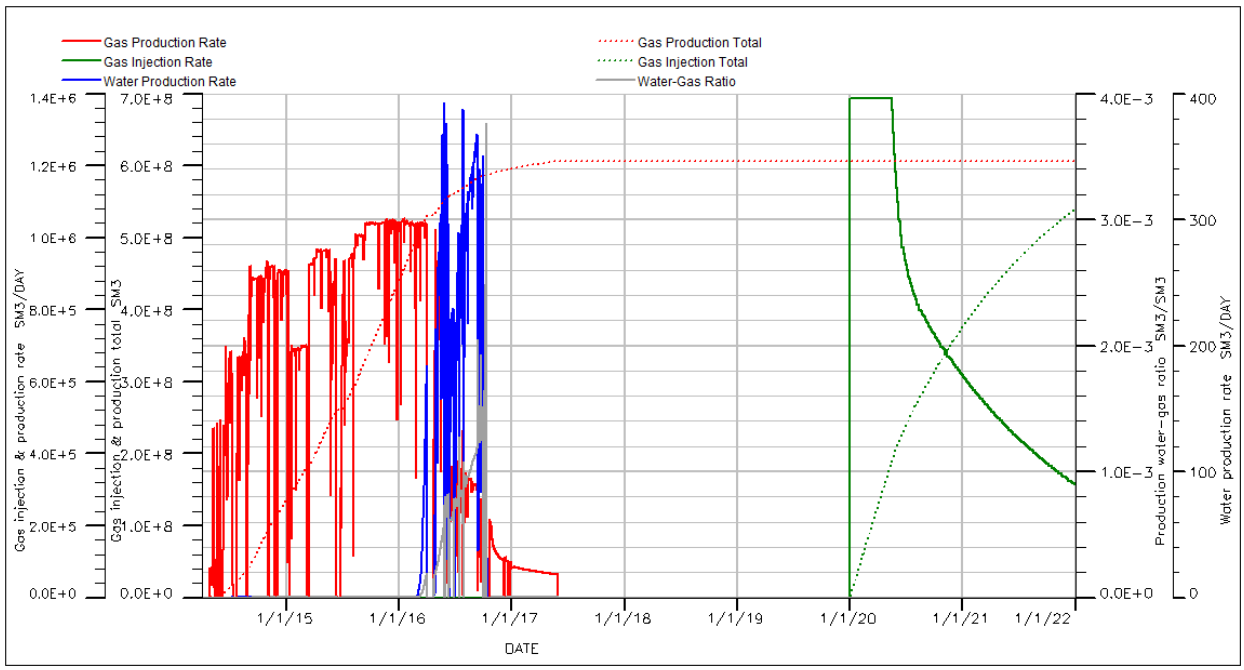

Prod. & Inj. profile for 0.93 pore volume factor and fit for purpose relative permeability curve

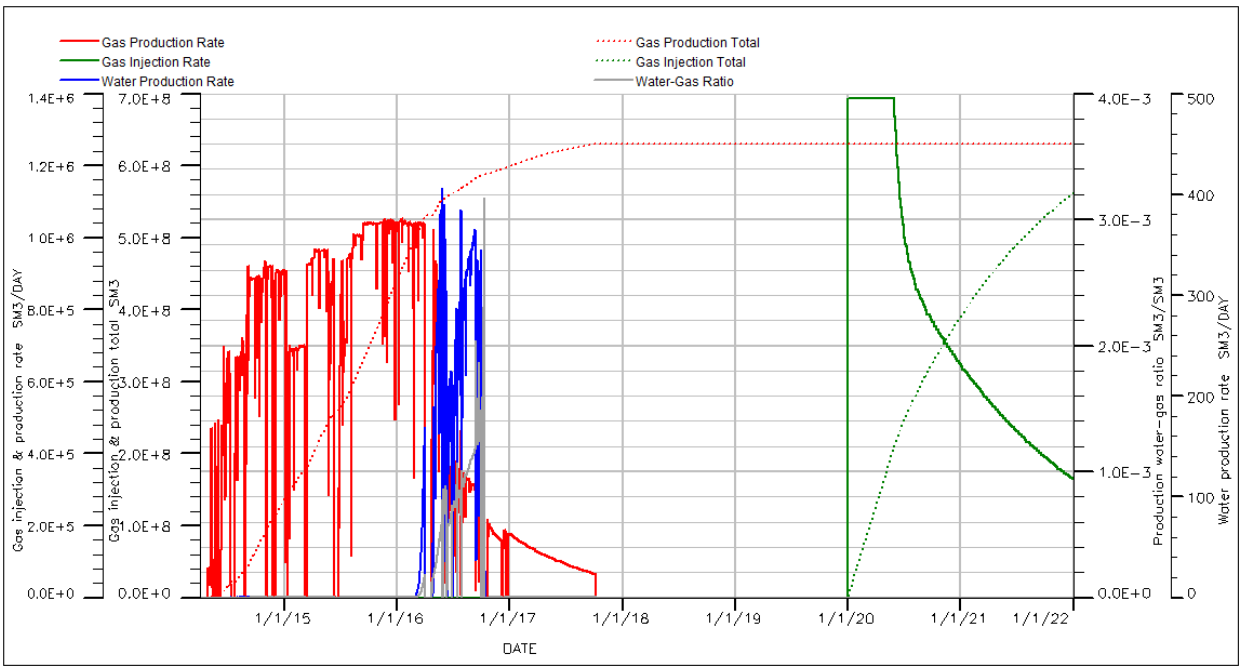

Prod. & Inj. profile for 0.96 pore volume factor and radial model relative permeability curve

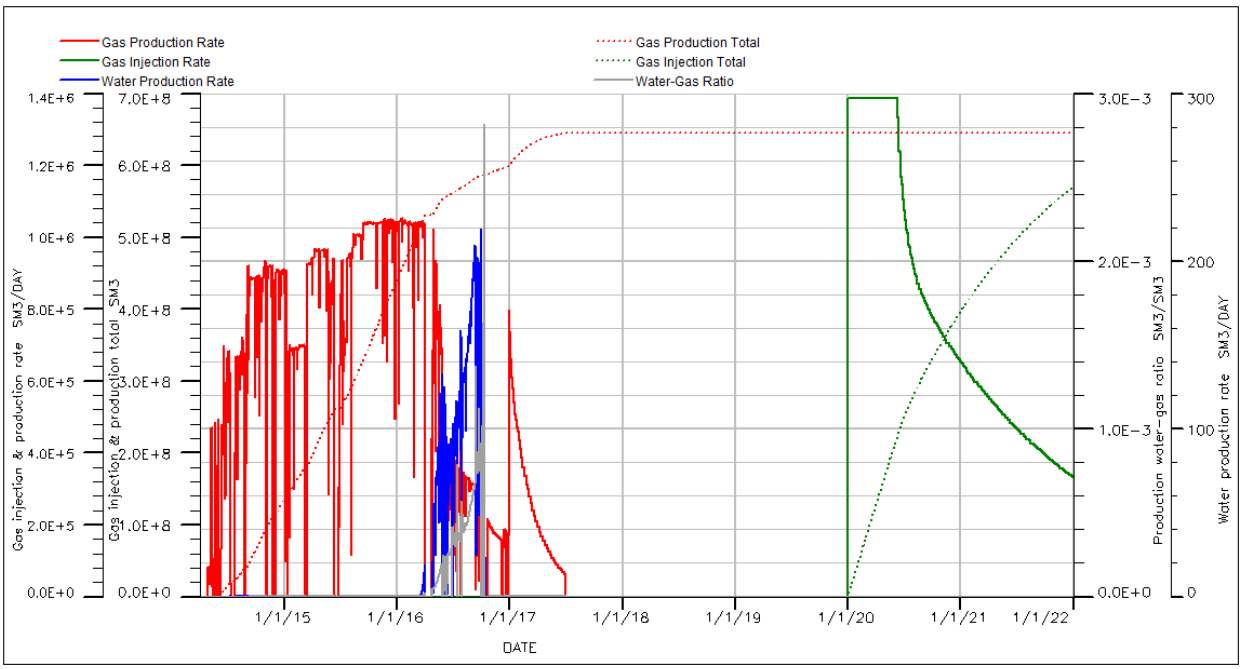

Prod. & Inj. profile for 0.96 pore volume factor and eclipse manual relative permeability curve

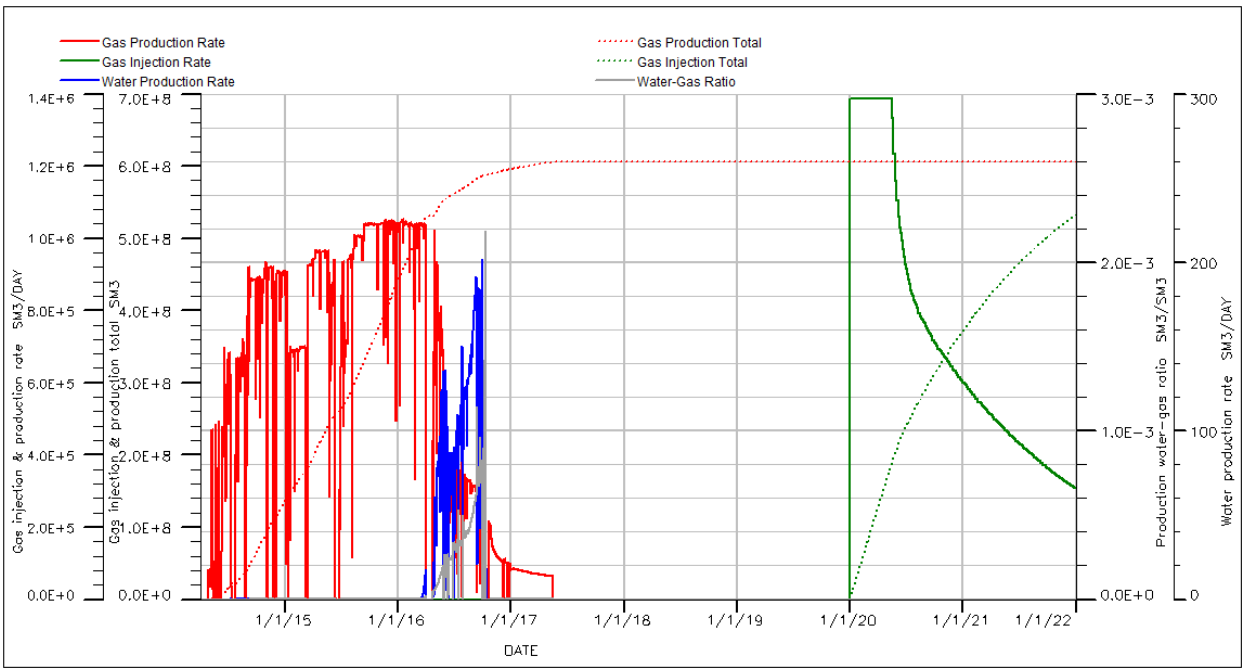

Prod. & Inj. profile for 0.96 pore volume factor and fit for purpose relative permeability curve

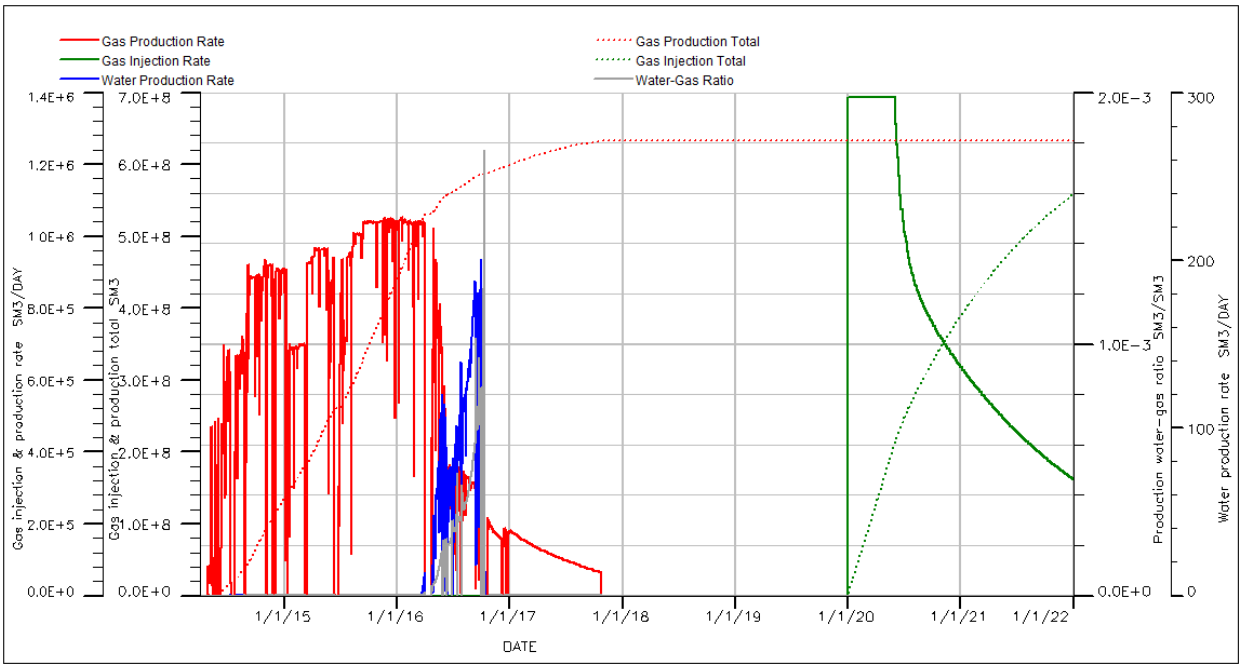

Prod. & Inj. profile for original pore volume factor and radial model relative permeability curve

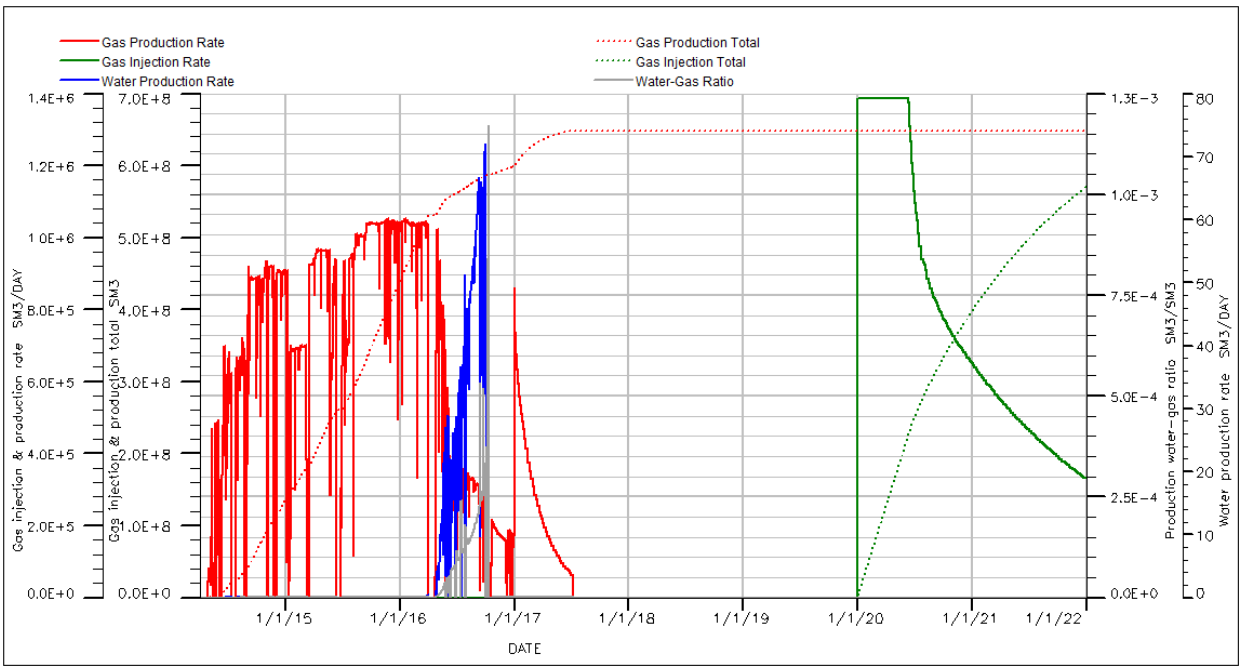

Prod. & Inj. profile for original pore volume factor and eclipse manual relative permeability curve

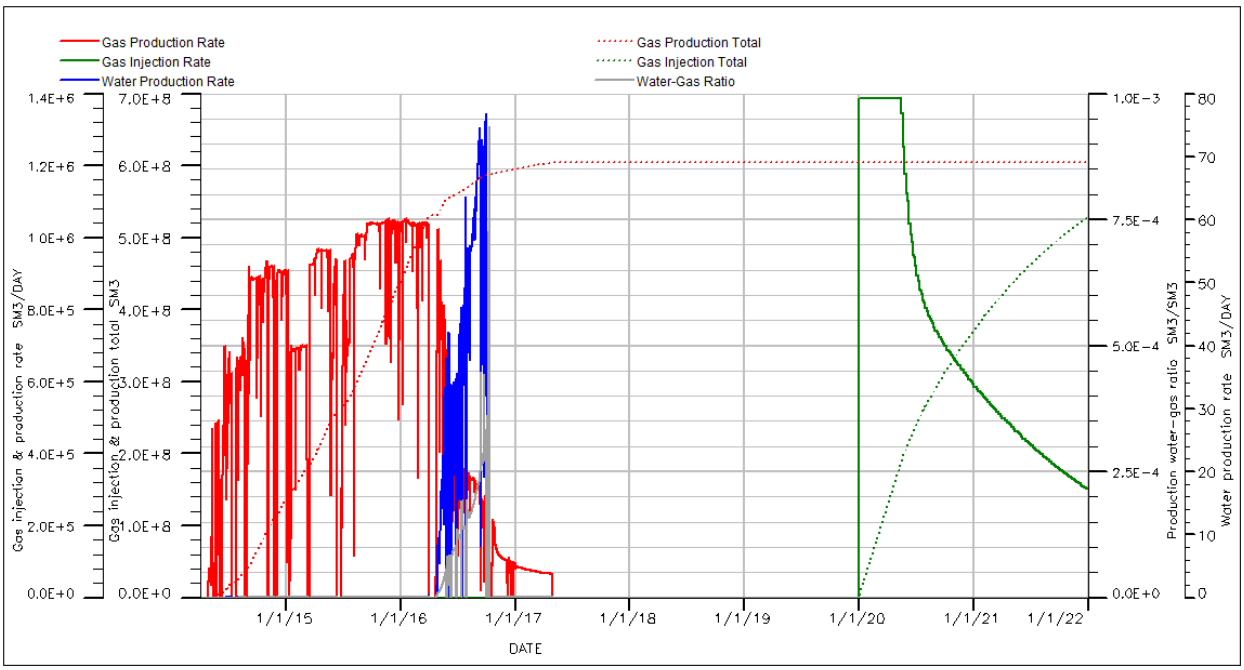

Prod. & Inj. profile for original pore volume factor and fit for purpose relative permeability